



Australia's National
Science Agency

Ultrasonic Assisted Drying and its Effect on 3D Printability of Minced Beef and Other Foods

11 October 2019

Viktor Lindström

Supervisor CSIRO: Henry Sabarez

Supervisor LTH: Björn Bergenståhl

Preface

This master thesis project was a collaboration between Lund University and CSIRO. The entirety of the time working with the project was spent at CSIRO's agriculture and food division, at the food innovation centre for industry in Werribee.

I would like to thank my examiner professor Marie Wahlgren and my supervisor professor Björn Bergenståhl at the Department of Food Technology under the faculty of Engineering, Food Engineering and Nutrition, Lund University for the help and guidance during the point that the opportunity to come to CSIRO was presented.

I would like to thank my supervisor at CSIRO, Dr Henry Sabarez from whom I learned a lot, who made sure that the work proceeded in the right direction and whose positive attitude was greatly encouraging.

The time at the site in Werribee was an absolute pleasure thanks to everyone at the site who welcomed me and never hesitated to provide a helping hand. Special thanks to Stephan, Thu and Jenny who went the extra mile to help me around the site.

Cite as: V. Lindström, Ultrasonic Assisted Drying and its Effect on 3D Printability of Minced Beef and other foods, Lund University.

Abstract

The aim of this master thesis project was to investigate the impact on drying kinetics of ultrasound during air drying by a new ultrasonic transducer, on which a patent application has been filed by CSIRO. Convection drying using hot air is currently the conventional method of drying in the industry due to its simplicity and low cost. To increase product quality, freeze drying utilises a vacuum but is highly energy consuming. The ultrasonic transducer is set to increase the drying speed, thus potentially replacing a need for the energy consuming vacuum. In this work, the effect the ultrasound had on drying kinetics of minced beef in 40°C and -15°C was examined.

The aim was also to investigate the 3D printability of meat dried using ultrasound. CSIRO wants to explore the possibility to increase low value food by drying it, potentially using an ultrasound assisted dryer, and then increasing the foods value by printing the long shelf life dried food. This would economically desirable both by increasing the price of the food, but also generating less waste since the dried food keeps substantially longer due the low water activity. To determine the effect ultrasound has on the printability, the formulation and rheological properties of a printable paste needs to be determined. Once completed, the printability of the meat dried with and without ultrasound could be compared.

The outcome of the work was that placing the sample on the transducer during drying at 40°C decreased the drying time by 40%. The decrease in drying time at -15°C could not be proved since the transducers cooling media was not flowing fast enough to cool it to -15°C. Viable methods and formulations for creating printable pastes using both xanthan gum and sodium alginate was established, however, the formulation will be affected by the minced beef used as a base in the paste. The meat dried at a colder temperature was more porous, and it was thus easier to reduce its particle size which is necessary for printing. The pastes created using meat dried at -15° also proved to have a slightly higher viscosity, is was thus determined that meat dried using colder temperatures was more favourable for printing. No difference was found in the beef dried with or without using ultrasound. Hence, implication of ultrasound during drying decreases the cost and the environmental impact, without affecting the product.

Table of content

Contents

1	Background	5
2	Aim	5
3	Disposition	5
4	Theory	6
4.1	Introduction	6
4.2	Hot air drying	6
4.2.1	Water activity	10
4.3	Vacuum Freeze drying	11
4.4	Ultrasound in Dryers	11
4.4.1	Ultrasound	11
4.4.2	Ultrasonic Dryers	13
4.4.3	Transducers	14
4.5	3D Food Printing	16
4.5.1	Introduction	16
4.5.2	Printing Meat	17
4.5.3	3D Printing	17
4.5.4	Binders	19
4.6	Rheology	23
4.7	Takayanagi Models	26
5	Method and Material	27
5.1	Objectives	27
5.2	Overview	27
5.3	Sample Preparation	28
5.4	Drying	29
5.4.1	Hot air drying	29
5.4.2	Atmospheric freeze drying	30
5.5	Moisture content	30
5.6	Milling	31
5.7	Screening trials	31
5.7.1	Screening: Paste Formulation	31
5.7.2	Screening: Printing	33
5.7.3	Screening: Suitable Thickener	34
5.8	Analysis Methods	34

5.8.1	Rheology measurement	34
5.8.2	Instron	34
5.8.3	Particle size measurement	36
5.8.4	Structure	37
5.8.5	Printing	37
5.9	Comparisons	37
5.9.1	Comparing: Amount of Thickener	37
5.9.2	Comparing: Takayanagi and Different Thickeners	37
5.9.3	Comparing: Particle Size Using Different Milling	38
5.9.4	Comparing: Particle Size Using Less Milling	38
5.9.5	Comparing: Dry and Wet Particles	39
5.9.6	Comparing: Drying Method	39
6	Results and Discussion	40
6.1	Drying kinetics	40
6.1.1	Hot air kinetics	40
6.1.2	Atmospheric freeze-drying kinetics	42
6.2	Losses of meat	44
6.3	Dried Meat	44
6.4	Results Screening Trials	47
6.4.1	Screening Trials: Paste Formulation	47
6.4.2	Screening Trails: Optimum Thickener	52
6.5	Results: Amount of Thickener	53
6.6	Results Takayanagi and Different Thickeners	57
6.7	Results: Particle Size Using Different Milling	58
6.8	Results: Particle Size Using Less Milling	60
6.9	Results: Dry and Wet Particles	61
6.10	Results: Drying Method	65
6.10.1	Drying Method: Rheology	65
6.10.2	Drying Method: Instron	67
6.10.3	Drying Method: Particle size	69
6.10.4	Drying Method: Structure	72
6.10.5	Drying Method: Printing	73
7	Conclusion	75
8	Further work	76
9	References	77

1 BACKGROUND

One of the major energy consumers during numerous industrial processes is the drying. To reduce the energy usage, production time and therefore also the cost of the process step, CSIRO has developed an ultrasonic transducer on which a patent application has been filed. The transducer is set to assist and facilitate convection drying at both higher and lower drying temperatures. Yet, further testing and determination of process parameters of the lab scale transducer is required before the technique is examined in a pilot plant.

CSIRO wanted to investigate the effect of drying using ultrasound had on the structural and nutritional properties of food. One possible future use of the ultrasonic assisted drying is 3D printing the product, therefore the printability of the differently dried foods was desired to be investigated. Minced beef was studied. The printability of the dried meat dried with or without ultrasound was investigated, for both higher and lower temperatures. To accomplish this, a method of producing a printable paste was developed in regards of particle size of the meat, meat to water ratio, type of additive, additive concentrations, homogenization method and printer settings. The chosen method would then be used to compare the differently dried meats.

2 AIM

The goal of this master thesis is to investigate the impact of ultrasound during convection drying on the drying kinetics using a new ultrasonic transducer on which a patent application has been filed by CSIRO. The effect on the drying kinetics of minced beef will be investigated and its impact in different temperatures.

The aim is also to investigate how different drying influences the product for 3D printing purposes, and to determine under which conditions dried meat can be 3D-printed. The optimum combination of properties will be sought after in regards of drying conditions, particle size of the meat, meat to water ratio, additive concentrations and type of additive.

3 DISPOSITION

The master thesis commences with a theoretical summary which includes information regarding drying kinetics and ultrasonic drying, followed by food 3D printing and food rheology. This is followed by a methodology and material section, presenting the work conducted. The results achieved and the discussion of these are followed by a conclusion and references.

4 THEORY

4.1 INTRODUCTION

One of the oldest and most commonly used methods of preserving food is the reduction of its moisture content. It is not only food that is being dried, but numerous industries are dependent on different drying methods in their process. Drying though is usually rather energy consuming, meaning that all reductions in energy requirements are both environmentally and economically desired. The effects of ultrasonic assisted drying have been known for years, but due to some problems as transferring the ultrasound efficiently to the product, the method has not yet been widely industrially implemented.

Drying food in colder temperatures is often necessary when a higher product quality is desired. Freeze drying is often implemented, a major drawback with this method though is that it is requiring a lot of energy to run. Implementing ultrasound instead of a vacuum pump might serve as a cheaper and more energy efficient option.

4.2 HOT AIR DRYING

The process of removing water from foodstuffs is one of the oldest ways of preservation, but it is also a highly energy consuming processing step. It has been estimated that drying processes in some places account for up 25% of the total energy consumption in the industry [1]. Many different drying methods are currently employed in the industry, but for many years convective drying utilising hot air has been the conventional method due to its simplicity and moderately low cost [1].

As straight forward as it may seem, drying is a rather complicated process with many factors affecting it, such as air velocity, air dry bulb temperature, air relative humidity, surface diffusion, capillary flow and the geometry of the sample being dried [2]. The drying rate can be described as the change of moisture over time, or:

$$\dot{m} = -\frac{M_s}{A} \frac{dX}{dt} \quad \text{Eq. 1}$$

Where M_s (kg) is the mass of dry solid, A (m^2) is the surface area in contact with drying medium and \dot{m} ($\text{kg}/\text{m}^2\text{s}$) is the drying rate that depends on the moisture content, X , and the drying conditions.

The relationship between the moisture content, X , and the drying rate, \dot{m} , is called the drying curve, $\dot{m}(X)$ which can be seen in figure 1. Several factors affect the drying curve, it is for instance necessary to investigate if the water in the solid can move freely or if it is bound by sorption.

The drying curve is mostly determined experimentally using constant drying conditions, the temperature, air velocity, total pressure and the relative humidity. The mass of the sample is weighed at a set time interval and the drying rate is obtained. At the first step of drying, the drying rate is virtually constant. In this step the unbound water in the solid is evaporated. When the water content is low enough, the surface of the solid dries out and additional drying takes place inside of the porous material. During the second drying step the drying rate is decreasing with the decreasing water content. This is due to the water still in the solid is bound by sorption. The third step is defined as the

water content between the maximum water bound by sorption and the equilibrium point of the drying [3].

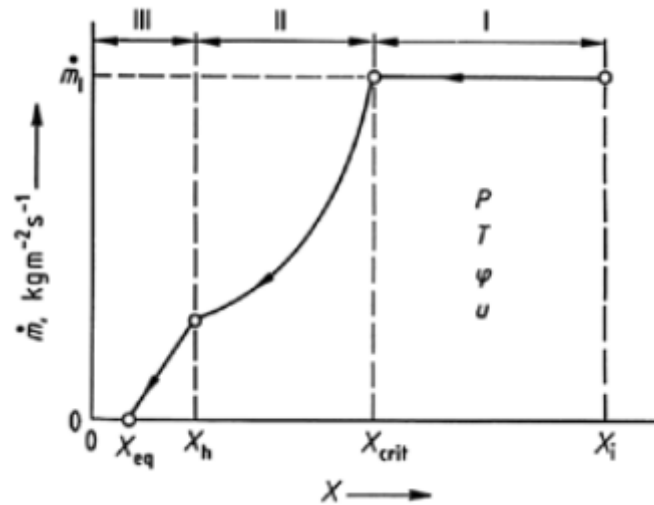


Figure 1 Example of drying curve, displaying the first, second and third drying step [3].

For free water, when it is contact with its own vapour, the vapour pressure is equal to the saturation pressure at that temperature. In the presence of air, the total pressure at the surface of the water is the sum of the saturation pressure and the partial pressure of the air, which can be written as:

$$P = P_v^*(T) * P_g \quad \text{Eq. 2}$$

Where P (Pa) is the total pressure, $P_v^*(T)$ (Pa) is the saturation pressure and P_g (Pa) is the partial pressure of the inert gas (often air).

The mole fraction of the respective constituent is equal to the partial pressure of the total pressure.

$$\bar{y}_V^*(T) = \frac{N_V}{N_V + N_G} = \frac{P_V^*}{P} \quad \text{Eq. 3}$$

Where N_V (mol) is the moles of water and N_G (mol) is the moles air.

Thus, the saturation moisture content of the air can be calculated as:

$$Y_T^*(T) = \frac{\bar{M}_V}{\bar{M}_G} \frac{P_V^*(T)}{P - P_V^*(T)} \quad \text{Eq. 4}$$

Where \bar{M}_V (g/mol) is the molar mass of water (18.01 kg/kmol) and \bar{M}_G (g/mol) is the molar mass of air (28.96 kg/kmol).

And the absolute humidity, Y (kg vapour/ kg inert gas) of the unsaturated air is calculated as:

$$Y = \frac{\bar{M}_V}{\bar{M}_G} \frac{\phi P_V^*(T)}{P - \phi P_V^*(T)} \quad \text{Eq. 5}$$

Where ϕ is the relative humidity, or:

$$\phi = \frac{P_V}{P_V(T)} \quad \text{Eq. 6}$$

If the water is bound to the solid by sorption, then it is not only the temperature but also on the moisture content will affect the absolute humidity of the air. In the gas-vapour mixture, the partial vapour pressure than the saturation vapour pressure. The equilibrium moisture of a solid can be shown as a function of the relative humidity of the gas at different temperatures, called sorption isotherms which can be seen in figure 2 [3]

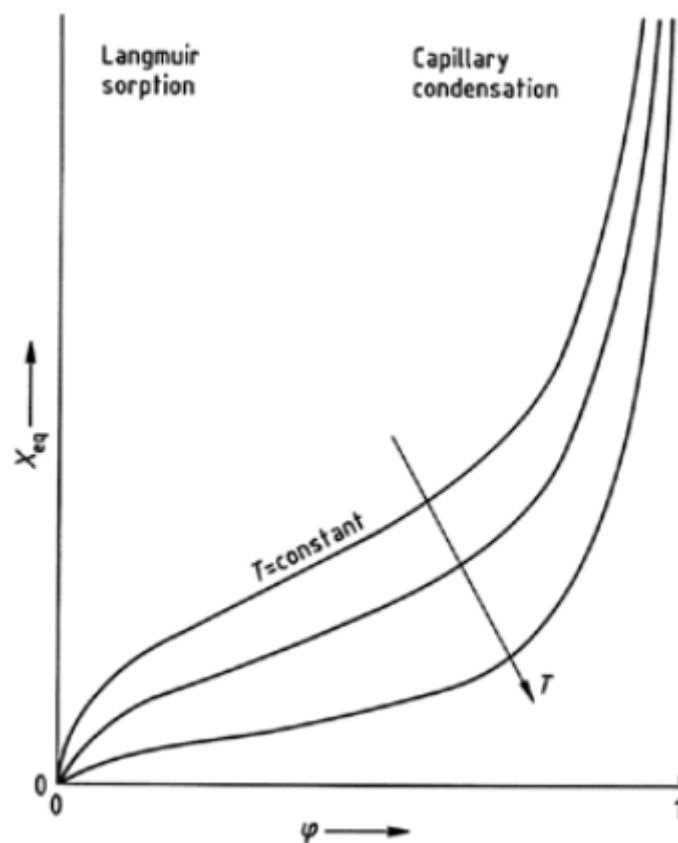


Figure 2 Example of sorption isotherms [3].

The two major phenomenon controlling water transfer from a solid are the internal flow of water from the inside of the material to the surface and the convective transport of water from the surface of the solid to the air, and the limiting phenomena will be the one controlling the drying speed, It is therefore necessary to find the optimum conditions for the process depending on the material [1]. To describe the diffusion of water from the inner regions in the solid to the boundary layer, Fick`s law of diffusion is often used because of its simplicity. The model assumes that the transport of liquid is due to the diffusion gradient, thus transporting the liquid to the surfaces of the material, and that the drying is conducted at a constant temperature. The model can be written as:

$$\frac{\partial X}{\partial t} = D \nabla^2 X \quad \text{Eq. 7}$$

Or for spherical coordinates for $r = 0$ as:

$$\frac{\partial X}{\partial t} = 3D \frac{\partial^2 X}{\partial r^2} \quad \text{Eq. 8}$$

And for $r > 0$ as:

$$\frac{\partial X}{\partial t} = D \left(\frac{\partial^2 X}{\partial r^2} + \frac{2}{r} \frac{\partial X}{\partial r} \right) \quad \text{Eq. 9}$$

Where D is the diffusivity (m^2/s), r is the radial coordinate, t is the time and X is the moisture content [4].

For long drying times the Fick`s equation can be simplified as:

$$\frac{M - M_e}{M_0 - M_e} = a \exp\left(\frac{-ct}{L^2}\right) \quad \text{Eq. 10}$$

Where a =empirical constant, dimensionless, c is the empirical constant (cm^2/h), L =slice half-thickness, M =moisture content, % dry basis (g water/100g dry solids), M_e = equilibrium moisture content, % dry basis, M_0 =initial moisture content, % dry basis and t is the time (s) [2].

The liquid is transported from the surface of the material to the boundary layer of air around it. The convective transport of water from the surface to the air is the external phenomena controlling the drying speed. The faster the air velocity, the smaller the boundary layer, and thus also the faster drying rate. Increasing the temperature of the air as well as the samples contact area with the air also increases the drying speed [5]. Exposing food at high temperature during longer times will affect the product quality negatively, meaning that aiding the water transport without the use of too much heat would be highly favourable for both the cost of the drying process and the quality of the product [1].

4.2.1 Water activity

Water is a necessity for many things in food products, as metabolism, growth and to aid carrying out many chemical reactions. Free water in fruits and vegetables, for instance, is among others supporting the microbial growth and acting as a transporting medium, while there are also water-soluble compounds that are binding water through osmotic binding. According to Raoult's law, this water-binding effect lowers the vapour pressure of the food. The water activity (A_w) is a comparison between the reduced vapour pressure and that of pure water at the same temperature.

Drying food, and thus lowering the water activity increases the shelf life of the food. This is because microorganisms that spoil the food or acts as pathogens require a high enough water activity to grow. Lowering the water activity therefore increases the shelf life, but only to some degree. Some water in the food will act as an antioxidant which means that lowering the water activity too much will increase lipid oxidation of the food as can be seen in figure 3 [6].

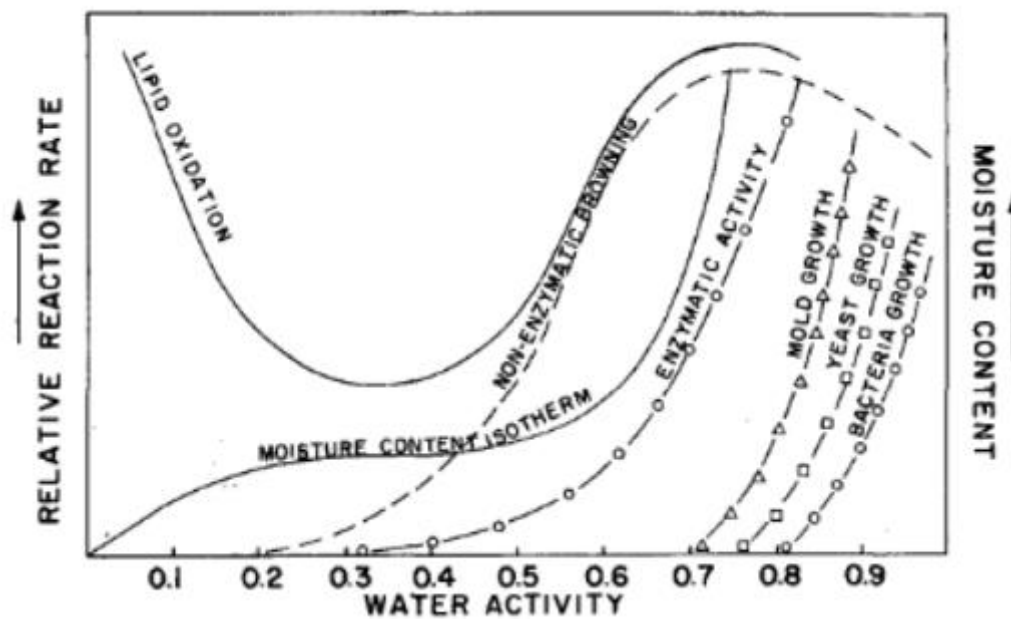


Figure 3 Water activity in relation to various reactions in food [6].

4.3 VACUUM FREEZE DRYING

Vacuum freeze drying is an alternative to hot air drying. The material during the process is first frozen, the water is then through sublimation under a vacuum extracted from the material and later condensed.

Freeze dried food is generally of a very high quality compared to food dried using hot air. The structure of the food during hot air-drying tends to collapse and thus reducing the porosity, the volume of the food and increasing the stickiness of dry powders. It has been observed that shrinkage during hot air drying can be extensive, around 80%, while using freeze drying it can range between 5 to 15%. The rehydration ratio is generally a lot higher as well in freeze dried foods, around 4 to 6 times higher [7]. Food can also be freeze dried in atmospheric pressure but requires severely greater drying times.

Browning and loss of colour is the result of various reactions during hot air drying. This does not only affect the visual aspect of the food, but also the amount of vitamins and antioxidants which are tightly linked to the colour.

The reason freeze drying is not used more in industry is because of the higher operating cost. It is estimated that running a freeze dryer costs 4 to 8 times more than hot air drying [7]. It is also a batch process with low through put that requires long drying times and some volatile flavours can be lost under the vacuum.

4.4 ULTRASOUND IN DRYERS

4.4.1 Ultrasound

Until quite recent, ultrasound in the food industry was used in similar fashions as in diagnostic forensics. The use was mainly analysing food properties, as droplet sizes in emulsions etc. Rather recently though, a new and more powerful form of ultrasound is being investigated and implemented in food processing [8]. Instead of the low energy and high frequency ultrasound used for analytical purposes, a high energy and low frequency ultrasound was already in the 1930s found to be able to among others, clean surfaces and the emulsifications of edible oils. The range the power ultrasound frequencies can be seen in *Figure 4*. More attention is now being paid to ultrasound techniques as recent research found the potential benefits for the food industry [9]. Today several institutes are developing their own ultrasonic transducer in order to claim market shares.

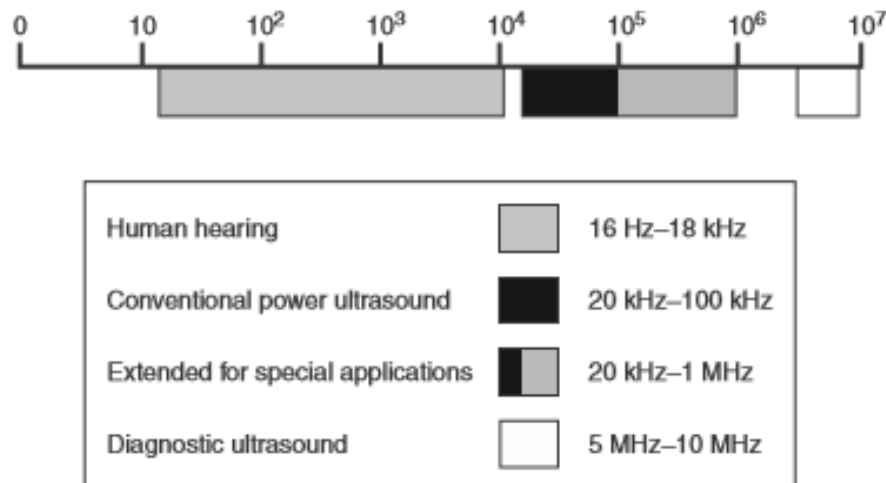


Figure 4 Classification of sound frequencies [10].

Ultrasound is a wave, the source of the sound causes vibrations that are transmitted to the adjoining particles. This way, the particles go through cycles of compression and rarefaction in the media in which it is propagating through. Ultrasound at high enough power can, traveling through water, cause cavitation bubbles or micro bubbles to form. The rarefaction cycle can be so intense that it exceeds the attractive forces in the liquid, in a sense the negative pressure is ripping the liquid apart, thus causing small gas bubbles to form [11]. In the cycles to come, the bubbles can collapse and upon doing so, releasing large amounts of energy around the micro bubble. The pressure during the collapse of the bubble is estimated to be up to several hundred atmospheres and temperature up in the thousands, creating local hot spots [9]. When the bubbles collapse, they do so with an extreme force and if the bubble is in contact with a surface, a sort of microjet hitting the surface is created. The shear forces in this microjet are extremely high and is the main effect observed when using high intensity ultrasound for cleaning purposes [11]. Though, the formation of cavitation bubbles during air drying can almost be neglected, making the heating effect less intense than in other applications [12].

When ultrasound is applied to a solid containing water, the effect of the contractions and the expansions has a similar effect of the one obtained when squeezing and releasing a sponge. This is referred to as the “sponge effect” and causes water bound in the inside of a material to be released and eases its transport to the surface of the material. The contraction and expansion forces can be so great that they overcome the surface tension, which keeps the water inside of the capillaries, thus forming microscopic channels inside of the material that makes it easier for the internal water to move [11]. The solid can also absorb the ultrasound and convert it into thermal energy through friction.

4.4.2 Ultrasonic Dryers

Applying ultrasound to a material being dried using a low temperature air stream has been known to enhance the drying speed since the 60s. This can either be done by applying airborne ultrasound with the drying air stream or applying it directly onto the material [9]. There are still limitations to both techniques though. So far, two major problems have halted the usage of ultrasound in gaseous dryers. There is a lot higher power loss when transmitting ultrasound through air than a liquid. There is also a mismatch between acoustic impedances between a gas and a solid, adverse to the transfer of acoustic energy from the air to the food being dried [8]. The direct contact ultrasonic drier provides higher efficiency, but a problem arises in the difficulty in combining it with existing hot air dryers. It has been found though that applying ultrasound to a drying process can decrease the energy consumption of more than 50% [13].

Fluidized bed drying experiments have found that applying ultrasound to a material being dried using low air velocities (< 6 m/s) greatly reduces the drying time of said material. The same did not apply for higher air velocities though. There was no effect on the drying speed found at all at air velocities of 12 m/s. Investigation of why these results were obtained showed that at high air flow rates, there was less acoustic energy in the medium. The high air flow rate disrupts the acoustic field generated in the chamber, and any turbulence further inhibits the effect. Lower air flow is in other words favourable for the propagation of acoustic waves in air [14].

Similar experiment was carried out to investigate the effect of ultrasound applied to drying at different air temperatures. In order to ensure a high acoustic effect, a low air flow rate was used. It was found that at higher air temperatures, the effect of adding the ultrasound to the drying disappeared. It was assumed that this was because when ultrasound is applied, the expansion and contractions in the material facilitate movement of the water. When the temperature increases, the water movement speed increases as well, thus making the relative effect of the added acoustic energy less influencing [14].

The effect of ultrasound had on different types of material were also investigated during drying. Carrot and lemon peel were looked at and a clear difference in the effects of ultrasound was observed. The effects were a lot stronger on the lemon peel than the carrot, which could be linked to the structure of the material. Lemon peel is considered more porous, meaning that it consists of more intercellular spaces, increasing the effect of the contractions and expansions thus facilitating the transport of water. The opposite can be found in carrots, where the small intercellular spaces produce a resistance to water transfer [15].

Experiments found that cell walls of material being dried with ultrasound had less structural deformation and collapse of the cells. The implementation of ultrasound while drying produced a product of higher quality, more like the fresh product. These results could be linked to the much shorter time exposed to the hot air [13].

4.4.3 Transducers

The general principal of a power ultrasonic process is based on an ultrasonic transducer which is driven by an electronic power supply. The vibrations are then transported by some media, some sort of solid coupling, a liquid or a gas, onto the material being dried. The principal can be seen in figure 5. The ultrasonic transducer can be constructed in many different ways. Earlier whistles and sirens where used, but that was before the wider implementation of piezoelectric ceramics which is now being the dominant transducer. More specifically, lead zirconate titanate piezoceramics [16].

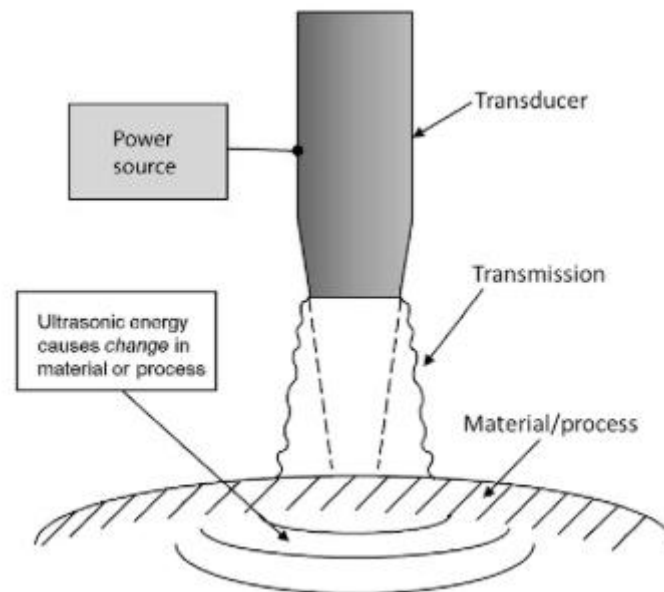


Figure 5 General power ultrasound system [17].

When designing a system to generate ultrasonic energy in a gaseous media, a problem needed to be overcome is the difficulty of sound propagation in low-density media. One way of doing so is using a larger radiator surface, but only to a certain degree. A too large radiator surface will not be able to vibrate in phase. The basic structure of a plate transducer can be seen in figure 6. It is generally constructed of a piezoelectrically activated vibrator that drives a larger radiator, fitted with a mechanical amplifier [14].

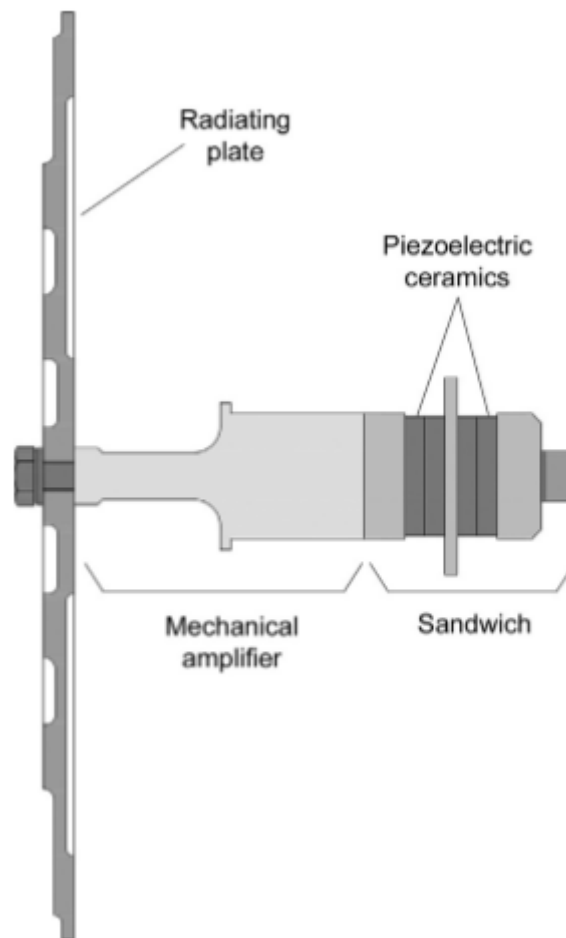


Figure 6 A schematic overview of a plate transducer [18].

Implementing a solution that would utilise and convey ultrasound in an effective way to the material and that could be combined with existing dryers would ensure that a lot less energy would be required during drying. Facilitating the drying would mean that less air, of a lower temperature would be used, not only saving money, but also the environment. The product will also be of a higher quality since it does not need to be exposed to high temperature for long periods of time and shorter production time will thus also be possible [13]. When focus lays on product quality and the need to dry in low temperatures, the method can thus be used instead of the highly energy requiring freeze drying.

A common problem with ultrasonic transducers is that they tend to get very hot, thus heating the sample being dried. This is undesirable since additional heating may affect the sample negatively since a lot of food is heat sensitive. Problems has also been identified as heat building up inside the sample by the friction created by the ultrasound.

4.5 3D FOOD PRINTING

4.5.1 Introduction

The interest for additive manufacturing, or 3D food printing, for food application has recently greatly improved. The possibility to affect, alter and customize the properties of food for one's individual needs is seen as a huge opportunity to meet the needs of special customers such as athletes, children and the elderly. The technique also makes it possible to revolutionise the way food is prepared at one's home. The 3D food printers have become a lot cheaper, meaning that it is now possible for larger majority of private kitchens to get them. This would greatly decrease both food loss and the preparation time of food, because the food could potentially be stored as a powder, greatly increasing the shelf life and thus decreasing food loss, and when desired it would be mixed with appropriate additives and simply put into the printer for preparation. This would allow the user to easily customize their meal in regards of shape, consistency, taste, content and nutritional value after desire.

The science of food 3D printing is advancing quickly, there is already a 3D printing restaurant and a lot of desserts and candy being printed. Research is being conducted in regards of if it is possible to incorporate alternative sources of nutrients into something more desirable for the general public, as insects as a source of proteins. Also, research is being conducted on the possibility to print entire sheets of muscle and fats, making it possible to print meat instead of using animal-based production [19].

There are several possible futures and uses for the technology of printing food. One idea is a monitoring system that is keeping track of one's dietary need and directly communicates it to printer that can prepare a meal suited to fulfil these needs. Or simpler, just providing consumer to have full control themselves over the nutritional content of their food. Another is providing people that are experiencing trouble swallowing solid food and thus requires food with paste consistency, such as people with dysphagia, food that is presented in the shape of food instead of paste.

Some industry has already started to implement 3D printing for large scale production. For instance, in the Netherlands there are now a factory 3D printing microwave pancakes, meaning that there might be a large increase in usage both for the industries and for private households [20].

4.5.2 Printing Meat

The general idea and concept of 3D printing a meat product out of meat powder is to add value to low grade meat by turning them into a desirable and functional product. Drying and grinding meat into a powder greatly decreases the water activity, thus also increasing the shelf life. This would decrease food waste since less food would be needed to be discarded due to spoilage. It would also decrease energy and money spent on transport since most of the weight in meat is water. The powder would be mixed with water and some sort of thickening agent into a paste, possibly directly in the printer, and then put in a cartridge. This could be done either by the consumer or the manufacturer, and then extruded into a shape chosen by the consumer. Different ways of cooking the extruded food is possible. Some existing 3D printers extrude the paste onto a hot plate, other cooking techniques involves more traditional cooking, like frying, once the printing is completed. If the meat has been properly pasteurised before the milling, potentially no further cooking would be required. The general concept can be seen in figure 7.

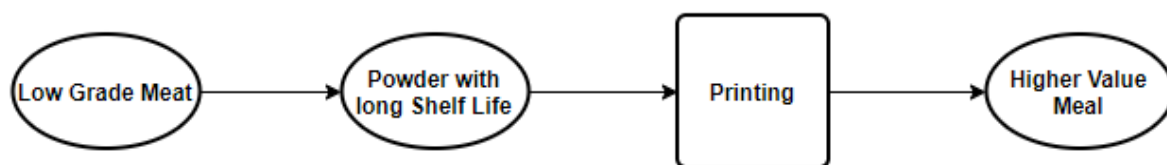


Figure 7 Flowchart of the general concept of 3D printing.

4.5.3 3D Printing

There are several different types of 3D printer available today. The extrusion 3D printing is based on a technique where a paste, mould or gel is extruded from a nozzle. Depending on the size of the nozzle, different levels of complexity can be achieved, but also affecting the total printing time of the product. The flow from the nozzle is controlled by either a motor, compressed air or a screw altering the pressure that the mould is extruded by. Once the mould has left the nozzle, it is desired that it solidifies to a degree that it will sustain any more mould that might be printed on top of it, thus allowing printing of 3 dimensional shapes as illustrated in figure 8. It has been found that many 3D printers design to print plastics easily can be modified for food printing instead because of their similarity in design [21]. Many printers use a Cartesian configuration of movement due to its simplicity in design, calibration and maintenance. The configuration has the printer head moving back to forth, left to right and up and down on an x, y and z axes which can be seen in figure 9.

Two significant strengths of 3D food printing are the possibility to produce highly complex geometric shapes and cheap production when producing small volumes of a product. This fits the food industry very well [19]. It is also possible to control the texture of the printed food. This can be achieved either by changing and altering the pattern the food is printed in, so that voids is incorporated into the product, increasing the porosity. It is also possible to print several materials with different textures together and thus affecting the mouth feel [19].

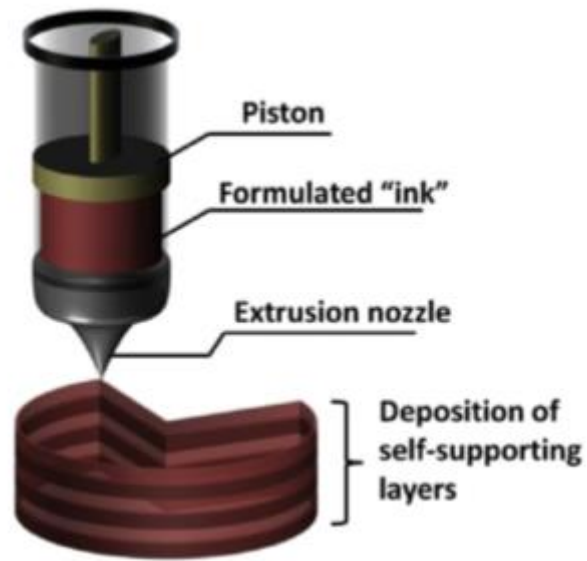


Figure 8 Illustration of extrusion 3D printing [22].

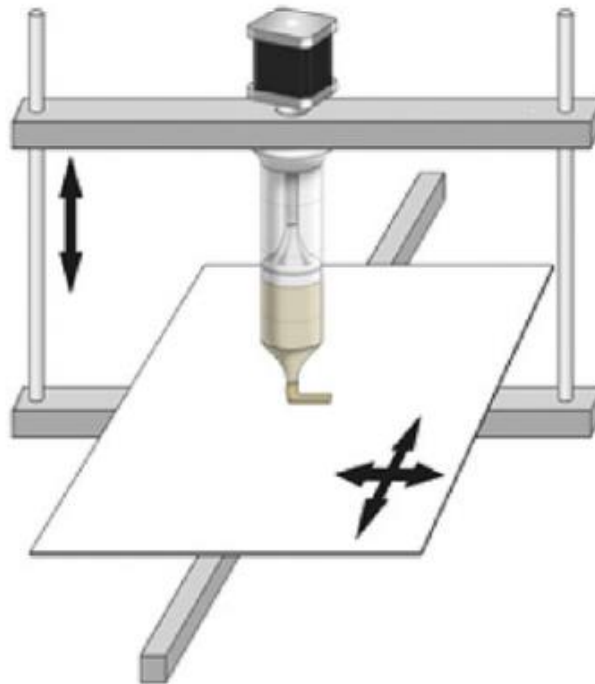


Figure 9 A Cartesian 3D printing configuration [20].

When printing soft food as pastes using an extrusion printer, the rheology of the material being printed is extremely important. The material needs to be soft enough for it to be easily and smoothly extruded and adhere to previously printed layers, but still hard enough to sustain its shape and carry the following layers being printed on top of it. A fluid with shear-thinning behaviour would then be ideal. At low shear stress, the fluid would be viscous enough not to flow from the nozzle by gravity, but when the extruder increases the shear stress the fluid would flow easily. When extruded, the shear stress would decrease, and the fluid would become more solid again in order to sustain the following layers to be printed on top of it. Having a fluid exhibiting too much shear-thinning behaviour with a high yield value though would mean that a high pressure would be needed to extrude the fluid and when applied, there would be risk of the fluid shooting out of the nozzle. Work therefor needs to be done in order prepare different foods to acquire properties that ensures that the printed shape is similar to the desired figure and that it remains intact after printing and potently cooking [23].

Additives such as sodium alginate, transglutaminase and xanthan gum in the food that will be printed can greatly increase the desired properties for food printing. It has been found the addition of 0.5% weight of transglutaminase to meat significantly increased the dimensional stability of the finished product [19]. The amount of additive also needs to be determined for different foods. Not enough will create a paste that cannot sustain itself, and thus will be inclined to slumping, and too much will make the gel strength too high, creating problem with the extrusion and making the product more prone to fractures [24].

For proper printing, especially for a fibrous material as meat, the particles in the paste needs to be finely comminute into much smaller particles. Mincing the meat can support the extraction of myofibrillar proteins that benefits stability of the formulated paste. As a guide line, the particle size of the printed paste needs to smaller than the printer nozzle to avoid clogging [25].

4.5.4 Binders

4.5.4.1 Transglutaminase

Transglutaminase is an enzyme that can be wildly found in nature in plants, fish and animals. It is involved in many biological phenomena, such as wound healing and blood clotting in animals. A while back, the enzyme needed to be extracted from animals, mainly guinea pig liver leading to small production rates. Now though a transglutaminase from *Streptovercillium sp.* has been isolated and are now being produced at low cost on a large scale by fermentation.

There are several ways that transglutaminase can modify proteins. They can alter the proteins by amine incorporation, crosslinking of proteins or deamidation which can be seen in figure 10. Studies now show that transglutaminase may have several uses in food production amongst others [26].

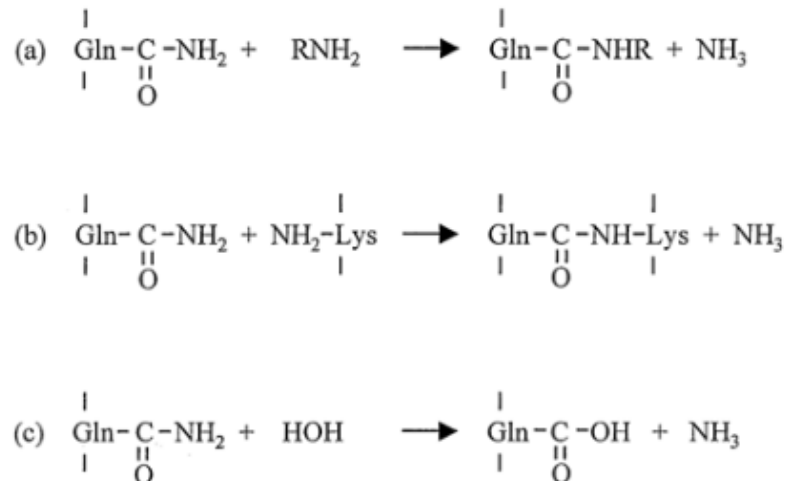


Figure 10 a: Acyl- transfer reaction, b: Crosslinking, c: Deamidation [27].

Transglutaminase expresses its highest enzymatic activity at a temperature of 50°C, but it still retained activity at temperatures just above 0°C. At higher temperatures of around 70°C it does not take long for the activity to go to zero. Transglutaminase is operating best at a pH between 5 and 9, which is the range used in most food processing processes. Unlike many other mammalian enzymes, transglutaminase derived from *Streptococcus* sp. does not require Ca²⁺ in order to display enzymatic activity. This is highly favourable in the food industry since Ca²⁺ is highly susceptible to many food proteins [26].

It has been found that transglutaminase improves the physical properties of meat when added. The addition led to a finer network structure of the meat that was not damaged by heat when the meat later was cooked, only the enzyme is deactivated by the heat. It is considered that the improved physical properties of the meat is because of the strengthened network structure. It was found that properties as firmness and elasticity were increased in both ham and sausage which can be seen in figure 11 [27].

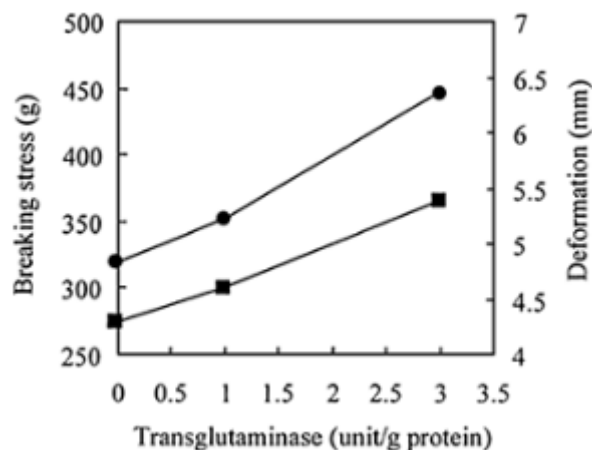


Figure 11 Breaking stress (circles) and deformation (squares) of sausage on addition of transglutaminase [27].

4.5.4.2 Sodium Alginate

Alginic acid is a polysaccharide that is found in abundance in the cell walls of brown algae. Together with metals as sodium, alginic acid form salts called alginates. Due to its origin, there is an abundance of it produced in nature. Despite it is being well used industrially, only a fraction of the bio-synthesised material is today being used, so increasing the usage would not pose difficulty. The possibility also exists to produce sodium alginate by fermentation, although the process is not yet economically feasible.

The purpose of the alginate in the algae is to provide both flexibility and structural rigidity. The alginate can look very different in different algae, and even in different parts of the same algae, and thus act as different structure-forming components [28].

The main application of sodium alginate in food production is to alter the rheology of the food, usually by the formation of a gel network by the interactions between the alginates and cations. Commonly, calcium cations are used to cross-link the polyatomic molecules, thus enabling the formation of a gel network. It is recommended that when alginates are to be mixed with salts that the alginates are hydrated before the addition of the salt under shear. It has been found that salt may inhibit the swelling of dry alginates. The reaction can be carried out at any temperature and is also unaffected by changes in temperature after the settling is complete, meaning that the gel structure will stay intact even after cooking of the product [29]. However, the properties of the finished product and the kinetics of the gelling process will be affected depending on the temperature that the gelling is conducted [28]. In order to control the properties of the food product that is produced, the rate of calcium released into the solution can be controlled and thus affecting the setting time and the properties of the food [29].

The alginate consists of two monomers, β -D-mannuronic acid (M) and guluronic acid (G). No regular repeating unit has been found, but it has established that the alginate consists of three separate fractions. Two of them consists of homopolymeric sections of mannuronic and guluronic acid. The third of a section containing both acids in nearly equal proportions as can be seen in figure 12. Due to this variation in structure and chain length of the polymer, the molecular weight becomes an average over the distribution. Commercial alginates though, have less variation in their composition.

Alginate is already used in food production and the usage is growing. Application today involves for instance the binding of flaked or milled foodstuff to make it look more like the original, mainly in meat products [28].

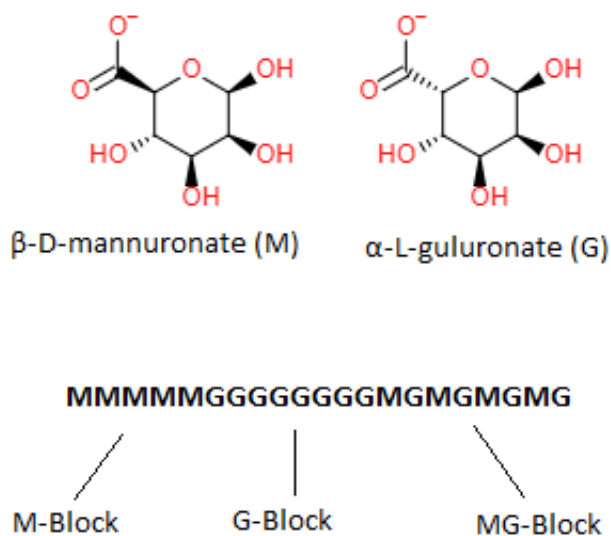


Figure 12 An illustration of a possible structure of sodium alginate.

4.5.4.3 Xanthan Gum

Xanthan gum is a food grade poly saccharide that currently has a wide range of uses in food, pharmaceuticals and cosmetics. Normal uses include salad dressings, dairy products and cosmetic creams which normally includes less than 1 w/w% of xanthan gum. In food it is commonly used as a thickener and stabilizer since water solutions are highly shear-thinning. The viscosity of a solution containing xanthan gum increases with increasing concentration and with decreasing temperature. The pseudoplastic behaviour of solutions with xanthan gum can enhance sensory qualities in food products and the three-dimensional structure formed can efficiently stabilize emulsions. To alter the desired properties, xanthan gum can be mixed with galactomannans like gellan gum. The hydrocolloids interact synergistically, thus enabling alteration of functionalities and reduced amounts needed.

The backbone of xanthan gum is similar to that of cellulose. It has a molecular weight around 2 million g/moles and is produced by fermentation, commonly by *Xanthomonas campestris* [30].

Solutions of xanthan gum exhibits pseudoplastic behaviour, as sheer-rate increases the viscosity decreases and it does this instantaneously. Xanthan solutions display no hysteresis, but it does show a primary yield stress than need to be overcome for it to flow [31]. The structure can be seen in figure 13.

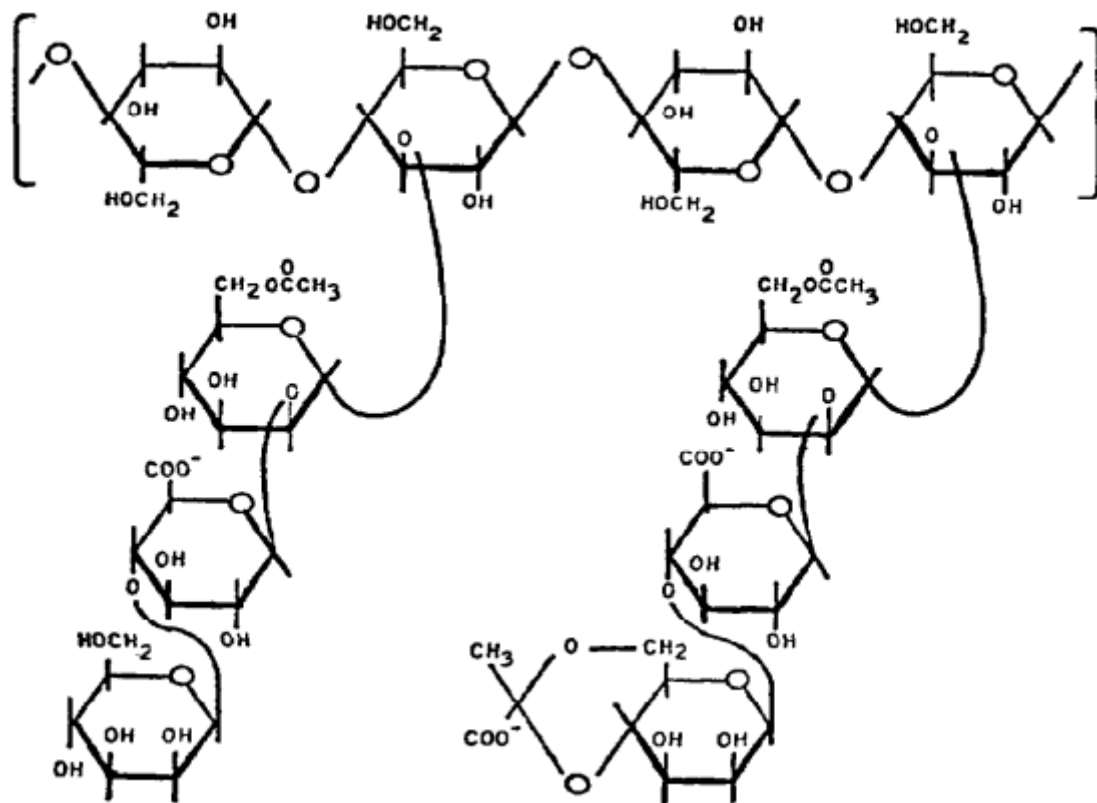


Figure 13 The structure of Xanthan gum [32].

4.6 RHEOLOGY

One of the most important factors in food is its texture. Depending on the type of food it can be differently important, but it is usually the food texture generally contributes a major part of how the food is perceived. The difference can easily be seen in the same type of yoghurt with the only difference is in how they have previously been processed, one pot set and one stirred. Same taste, but completely different mouthfeel [33]. When a food additionally will undergo printing, the texture and rheology of the food become of even further importance. Fluids, such as water, that has viscosities that are not affected by the fluid conditions are called Newtonian fluids. Many fluids though are not Newtonian, especially different foods because they may contain large particles or long-chain molecules which interactions may be dependent on how the material is deformed. Fluids whose viscosity alters depending the previous and present conditions of the system is called non-Newtonian. Adding thickeners such as xanthan gum to water-based products can make the food appear thicker, which in the right concentration can be perceived by the consumer as higher concentration and therefore be desirable. Too high concentration of thickener though might make the product undesirably thick and less pleasant to consume.

Fluids in motion withstand shear stress, which act tangentially to plan. An example of shear flow can be seen in figure 14, the fluid is sheared between the stationary bottom plane and the moving plane with a distance of a . The shear stress can be calculated as:

$$\tau_{xy} = \mu \dot{\gamma}_{xy} = \mu \frac{dv_x}{dy} = \mu \frac{v}{a} \quad \text{eq. 11}$$

Where τ_{xy} (Pa) is the shear stress in the fluid, $\frac{dv_x}{dy}$ (m/s) is the velocity gradient, μ the coefficient for viscosity (Pa*s) and $\dot{\gamma}_{xy}$ (1/s) is the shear rate.

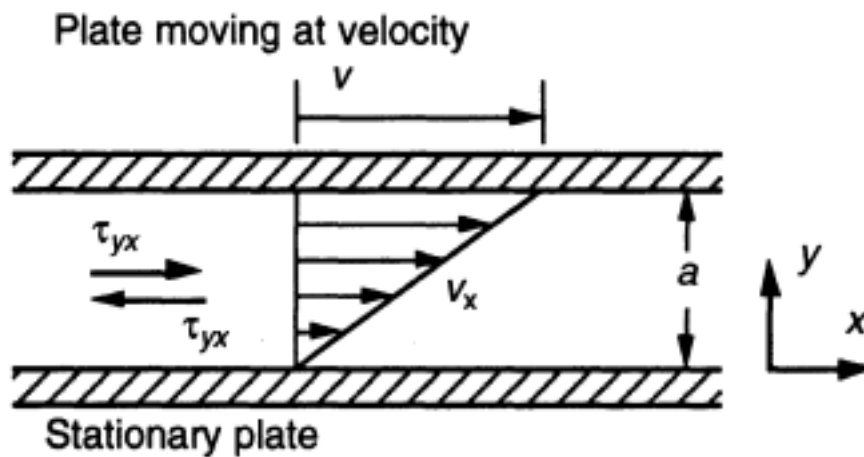


Figure 14 The flow between 2 parallel plats, the top moving at velocity v [34].

For non-Newtonian fluids the apparent viscosity, $\mu_a(\dot{\gamma})$, can be calculates as:

$$\mu_a(\dot{\gamma}) = \frac{\tau}{\dot{\gamma}} \quad \text{eq. 12}$$

How different types of non-Newtonian fluids behave in regards of sear stress and rate can be seen in figure 15 [34].

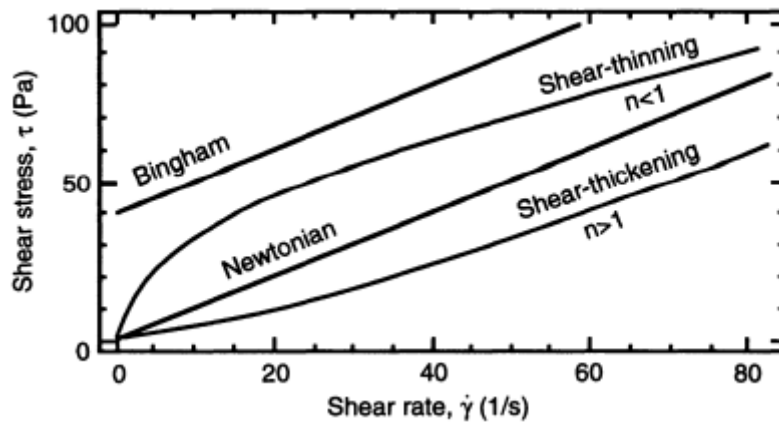


Figure 15 Flow curves of Newtonian and several non-Newtonian liquids [34].

The apparent shear stress in a tube can be calculated as:

$$\tau = \frac{r \cdot \Delta P}{2L} \quad \text{eq. 13}$$

Where r (m) is the radius of the tube, L (m) the length of the tube and ΔP (Pa) the pressure-drop.

One way to calculate pressure drop in a tube is:

$$\Delta P_f = 4f \frac{L}{D} \frac{\rho \bar{v}^2}{2} \quad \text{eq. 14}$$

Where L (m) is the length of the pipe, D (m) the diameter of the pipe, ρ (kg/m^3) the density of the pipe, \bar{v} (m/s) is the velocity and f the Darcy friction factor. The Darcy friction factor can be determined by the Reynolds number using the Moody diagram [35].

Under the assumption that the fluid is Newtonian, the apparent shear rate in a tube can be calculated as:

$$\dot{\gamma} = \frac{4Q}{\pi r^3}$$

eq. 15

Were Q (kg/s) being the laminar volumetric flowrate in a circular tube and r (m) is the radius of the tube [36].

4.7 TAKAYANAGI MODELS

Many interpenetrating polymer mixtures are phase separated, often into on rubber and plastic phase. The Takayanagi models aid to better understand and explain the mechanical properties and behaviour of polymer networks. Some combinations of the models can be seen in figure 16. The morphology and the phase continuity will have great impact on polymer networks the mechanical behaviour. When the rubbery phase is continuous and the plastic dispersed, the mixture will be softer and when the plastic phase is continuous and the rubbery dispersed the mixture will display more rigid behaviour. Thus, the continuous phase will dictate many of the mechanical properties of the mixture [37].

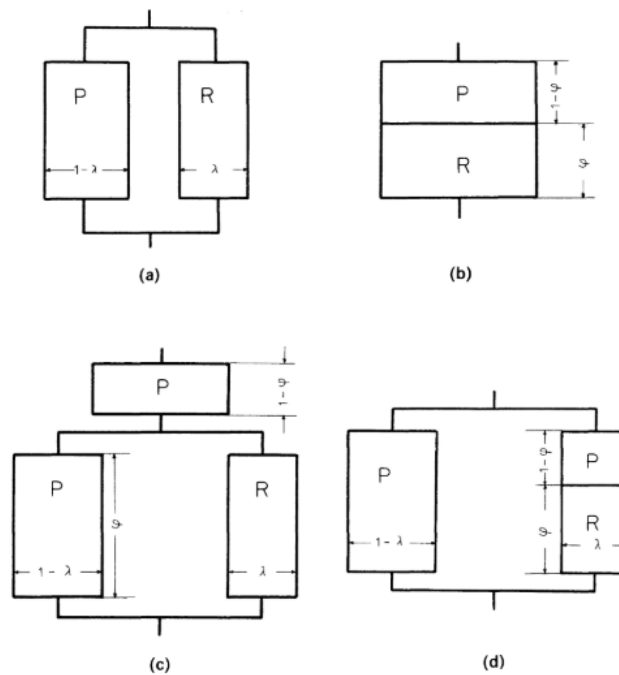


Figure 16 Takayanagi models for a 2 phase polymer network. R represents the rubber phase and P the plastic. (a) and (b) illustrates the parallel and the series model. Combinations of (a) and (b) are illustrated in (c) and (d) [38].

5 METHOD AND MATERIAL

5.1 OBJECTIVES

The work conducted sought to determine how the newly developed ultrasonic transducer affected the drying kinetics of convection drying at different temperatures. To accomplish this, the sample meat needed to be prepared as it would when used industrially. The drying kinetics were chosen to be investigated at 2 temperatures: 40°C and -15°C. For both temperatures one sample was dried with ultrasound and one without, this while measuring any potential heating effect from the transducer that would affect the drying kinetics.

It was also desired to determine if drying using ultrasound affected the product for 3D printing purposes. To determine this, initially a method of preparing a printable paste of dried meat needed to be established. This included determining and comparing the milling method of the dried meat, the meat powder to water ratio, using xanthan gum or sodium alginate, the additive concentrations, the homogenization method and the printer settings. Once a viable paste formulation had been determined, the effect of the different drying methods of the meat could be determined in terms of its viscosity and shear thinning behaviour.

5.2 OVERVIEW

A rudimentary overview of the process used during the work from minced meat to a finished meal can be seen in figure 17.

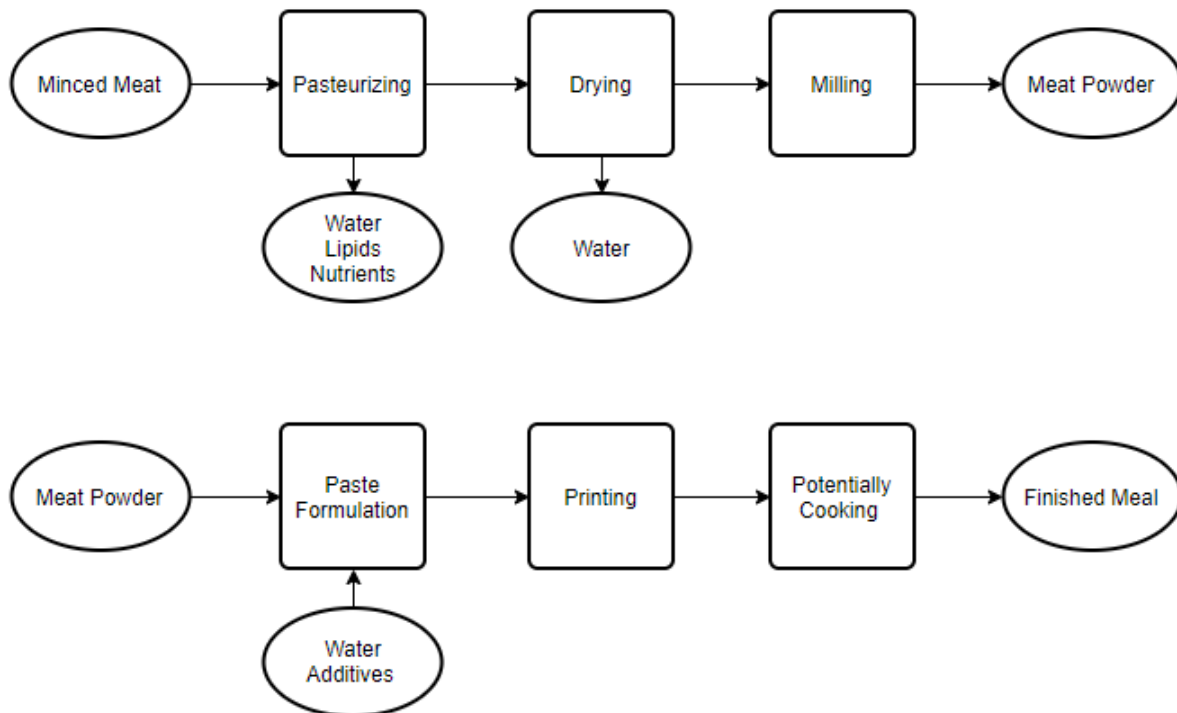


Figure 17 A flowchart of the process from minced meat to finished meal.

5.3 SAMPLE PREPARATION

Beef mince, extra lean, was purchased from the supermarket chain “Coles” and stored at 5°C. The meat was put into trays, weighed and then put in a water bath at 85°C for 10 minutes, with a stir after 5 minutes, to extract fat and kill microorganisms. The meat was then rinsed with cold water to abort the cooking and drained with a cheese cloth. The meat was then put back into the tray and the weighed again. This procedure was repeated 4 times with a change of the water in the water bath after the second repetition, this to reduce the lipid concentration in the water bath to further extract fat during the pasteurization. 4 trays were fitted with a Tinytag Plus 2 temperature and relative humidity sensor from GDL each, logging the temperature continuously to see if the sample got heated by friction from the ultrasound. Around 500 grams of the meat was added to each tray. 3 samples of fresh and 3 samples of cooked meat were weighed. These were placed in an oven at 105°C for 24 hours, this to determine the water content of the meat and therefore provide an indication on when the drying was complete and how much moisture the meat contained before the drying.

5.4 DRYING

5.4.1 Hot air drying

The air drying was carried out using a test dryer with a schematic diagram can be seen in figure 18. The dryer enabled full control over process conditions as temperature, air flow and humidity. The dryer was also fitted with several different sensors interfaced with a computer-based data gaining and control system for recording of the conditions during the process.

The drying conditions was set to an air temperature of 40°C, 25% relative humidity and an air velocity of 1.1m/s. Immediately after sample preparation, 2 trays were put on the ultrasonic transducer fitted with a plastic conveyor belt due to potential heating from the transducer and more accurately to mimic industrial use (H+US) and 2 trays were placed away from the transducer (H-US). The 2 specimens dried with ultrasound were named (+US1) and (+US2) and the 2 without (-US1) and (-US2). The transducer utilizes direct contact with the sample being dried but to reduce the potential heating from the transducer, which usually occur in ultrasonic transducers, a cooling media is run underneath the contact surface thus cooling the contact area with the sample. It is then only the ultrasound affecting the drying process. With the transducer the ultrasonic transducer the drying can be run continuously. The transducer was set to 100% power corresponding to 2kW at a frequency of 40kHz.

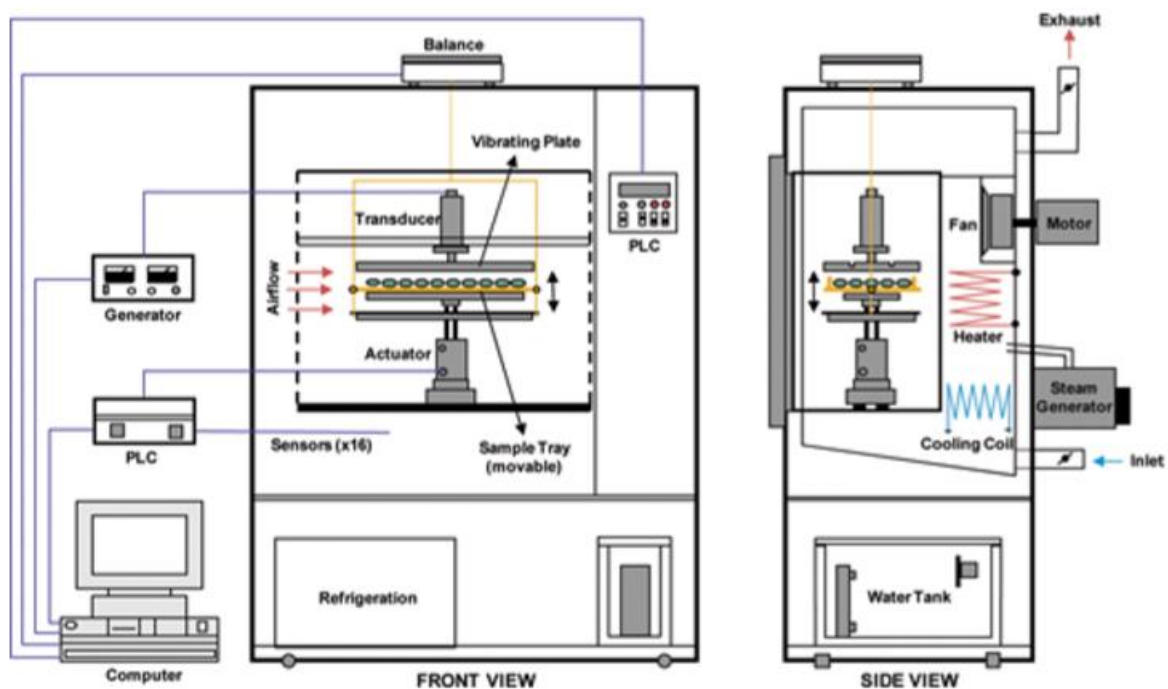


Figure 18 Schematic of the ultrasound assisted drying setup [13].

5.4.2 Atmospheric freeze drying

After sample preparation, the samples were placed into a freezer of -18°C over the weekend. The layer of meat was kept as thin as possible, this because the ultrasound has a heating effect by vibrations that are converted into heat. Maintaining a thin sample increased the meats contact with the cold air, minimizing a rise in temperature. The temperature sensor was placed to detect any rise in temperature inside of the meat samples.

The weight of both trays was determined, and both put into a freezer at -15°C to simulate drying below freezing conditions. One tray was placed on an ultrasonic transducer (C+50% US) fitted with a plastic conveyor belt to prevent any potential heating from the transducer and to more accurately mimic industrial use, and one was placed near the transducer (C-US). The ultrasonic transducer was set to 50 % power corresponding to 1kW at a frequency of 40kHz and a refrigerant cooling flow of 300 ml/min of -10°C . The reason not higher power was used was due to problems in the cooling. The pump could not transport the refrigerant fast enough to properly cool the transducer, thus the transducer would heat the meat above the desired temperature. A more efficient pump was ordered but did not arrive in time to be utilized during the trial. At the end of drying, the power of the transducer needed to be increased to 75% to further the evaporation to a desirable moisture content and the conveyor belt was removed at this time.

After 70 days, the meat dried without ultrasound was still not dry enough. The samples were then dried to a desirable moisture contentment in a vacuum drier. The pressure was set to 2342 μBar and the shelf temperature to 16.7°C . The high temperature was due to that the cooling system was malfunctioning.

5.5 MOISTURE CONTENT

The initial moisture content of the meat was determined by taking samples from each of the meat packages used, mixing them and then storing at 100°C for 24 hours. 3 replicates were done to obtain a representative average. The moisture was expressed on a percentage wet basis (kg water/kg wet sample * 100). It was found that the meat had an initial moisture content of around 73.82% fresh and 68.67% moisture after pasteurization.

The moisture was also determined in the differently dried samples. This by storing a sample at 100°C for 72 hours and weighing before and after. 2 replicates were done. The moisture was expressed on a percentage wet basis (kg water/kg wet sample * 100). The moisture contents can be seen in table 1.

Table 1: Moisture contents of the differently died meats samples.

Drying Method	Moisture content (average of the 2 samples)
Hot air without ultrasound	13.09 weight%
Hot air with ultrasound	13.52 weight%
Cold air without ultrasound	6.85 weight%
Cold air with 50% ultrasound power	7.15 weight%

5.6 MILLING

A standard milling procedure was developed to both ensure that the particles was small enough to mix with water and not block the nozzle of the 3D printer. It was also necessary to make sure that the milling was performed in the same way every time for the process to repeatable. Several different methods were evaluated before one was chosen.

The dried meat was kept cold and directly put into the GM200 rotating blade food processor from Retsch for 5 seconds at 10 000 rpm to break up larger particles. Afterwards, the meat was run through the Pulverisette 14 Rotor Speed Mill from the company Fritch. The mill was set to a speed of 6 000 rpm and a 0.2 mm sieve ring was used. The meat was weighed before and after the milling to determine losses.

5.7 SCREENING TRIALS

The literature study provided scattered information on the required and preferred concentrations of the thickening agents in relative the water to solid ratio for proper printing properties in the gel. Furthermore, different meat powders can vary in their properties, thus not being optimal for every mix of thickening agents. Therefore, screening trials were primarily conducted, starting from the concentrations provided in literature, and then fine-tuning the parameters for the best results. This was also done to find the optimum particle size and the best thickening agent of either sodium alginate or xanthan gum. The analysis was preformed visually, and the properties of the best ones were later more thoroughly analysed in regards of rheology.

5.7.1 Screening: Paste Formulation

A standard procedure was developed for formulating the paste. It followed: Depending on the chosen ratio of meat to water, the appropriate amount of consistently tempered water was poured in a beaker. Then, the chosen amount of the thickening agent was added. The mixture was homogenized with a household blender called StickMaster Plus from the company "Sunbeam" for 5 seconds. The meat powder was added to the mixture and the StickMaster Plus was used again for homogenization, 30 seconds at speed level 1 and 30 seconds at level 2. In between the runs, a spoon was used to scrape of any dryer parts stuck to blender. The manufacturer of the StickMaster Plus unfortunately did not provide information on the speed of the different levels, so the shear rates could not be determined.

Finally, the paste was sieved through a tea sieve. A spoon was used to scrape the paste through. The sieve caught any potential larger particles that might have clogged the nozzle of the printer and further reduced the particle size of the paste.

To determine the appropriate thickening agent for the investigation, trials using 2 different thickening agents combined with hot air-dried meat was done. The thickening agents used was xanthan gum and sodium alginate combined with calcium carbonate and an acidifier. Both were mixed with the standard procedure, except that for the sodium alginate the calcium carbonate was added after the addition of the sodium alginate and the acidifier (Lactic acid, 9%) was added during the homogenisation. Adding the lactic acid rapidly enhanced the solubility of the calcium carbonate, thus increasing the viscosity of the paste by facilitating cross linkage of the sodium alginate. Concentrations was collected from literature, tested and then altered for optimum printing using the meat provided [30] [25]. The effect of printing newly formulated paste and letting it set over night at 5°C was also investigated. The different prints were visually and texturally compared, and the optimum blend for each of the 2 thickening agents were then determined. The concentrations investigated can be seen in table 2 and 3.

After some trials, the printing speed chosen was 100% of the printer's maximum, which on an average was 0.48 mm/min or 1.83 cm³(paste)/min. Printing in lower speeds proved easier, so it was decided that pastes needed to be able to be printed at the highest speed possible.

Table 2: Concentrations for paste formulation using sodium alginate, calcium carbonate and lactic acid.

Sample name	Meat : Water (weight)	Sodium alginate (mM, weight% to water)	Calcium carbonate (mM, weight% to water)	Lactic acid (mM, weight% to water)
(3)	1:2.5	46.3, 1%	-	-
(4)	1:2.5	92.54, 2%	-	-
(7)	1:4	46.3, 1%	-	-
(8)	1:4	92.54, 2%	-	-
(9)	1:2.5	69.41, 1.5%	-	-
(10)	1:2.5	57.84, 1.25%	-	-
(11)	1:3.3	69.41, 1.5%	100.6, 1%	67.8, -
(12)	1:2.5	34.7, 0.75%	50.12, 0.5%	6.78, 0.5%
(13)	1:4	34.7, 0.75%	50.12, 0.5%	6.78, 0.5%
(20)	1:3.3	34.7, 0.75%	50.12, 0.5%	6.78, 0.5%
(21)	1:3.3	46.3, 1%	50.12, 0.5%	6.78, 0.5%
(23)	1:3	34.7, 0.75%	50.12, 0.5%	6.78, 0.5%

Table 3: Concentrations for paste formulation using xanthan gum.

Sample name	Meat : water (weight)	Xanthan gum (mM, weight% to water)
(15)	1:4	0.005, 1%
(16)	1:3.3	0.005,1%
(17)	1:3.3	0.006, 1.25%
(18)	1:3.3	0.008, 1.5%
(19)	1:3.3	0.010, 2%
(24)	1:3.3	0.013, 2.5%
(25)	1:2.5	0.010, 2%
(28)	1:2.5	0.013, 2.5%

5.7.2 Screening: Printing

The printing was done by a 3D printer called “Focus” by the company “ByFlow”. It is a portable, easy to use and easy to start printer. The printer has two exchangeable printer heads that are magnetically attachable, it recognises which one is attached and alters its settings accordingly. One printing head has a heated nozzle, allowing it to print filaments and the other is made for pastes. The printer is printing onto a plate that can be heated, thus allowing cooking of food paste as it is printed.

3D models for the printer can be uploaded via a WIFI connection. Some models are already available on the printer. New ones can be uploaded as G-files. These can be generated by a software called Slic3r. The 3D models can be generated in 3D programs like TinkerCAD or AutoCAD and then they need to be uploaded to Slic3r as a STL-file.

First the paste needs to be filled into a cartridge, this in the absence of any bubbles or air pockets left inside. This would result in that air would be extruded during the printing, resulting in holes or missing parts in the finished figure. The cartridge is loaded into the 3D printer and the desired printing speed is set. Usually, higher printing speeds can result in more problems during printing as “dragging”, where the paste has not been connected properly to the previous layer before the nozzle moves away, resulting in paste dragged away from the desired position. Dragging might also occur when the nozzle height is larger than optimum. When it is smaller than optimum, the paste might end up scattered thus expanding the desired design. When this is set, the desired figure is chosen.

For this project, the figure chosen was one called the “Gecko”. This due to the figure’s complexity, height and detail. The nozzle used had a circular opening with a 1.6 mm diameter.

5.7.3 Screening: Suitable Thickener

The analysis on what concentration of thickener in combination with what ratio of meat to water was performed visually and by manually examining the resulting figures. First, appropriate concentrations and ratios were determined the 2 thickeners, followed by that the most suitable of the one prepared with Xanthan gum or Sodium alginate was chosen.

5.8 ANALYSIS METHODS

5.8.1 Rheology measurement

To study the rheological behaviour of the pastes, measurements were performed in the Rheometer: MCR 301 from Anton Paar using the RheoCompass software. The measuring system was a cup (diameter of 28.92mm) and a vein (diameter 22mm and length, 16mm). 2 different programs were used: the first a ramp log increasing the shear rate from 0.001/s to 3000/s and the second had a constant shear rate of 0.001/s. The rapid decrease in shear rate in the second program would provide data regarding the speed that the pastes regained their viscosity. Both tests were conducted at 20°C. Before the start of the measurements, the equipment was set up according to the specifications from the manufacturer.

5.8.2 Instron

The material testing frame Instron 5564 combined with the Bluehill 3 software was used to measure the force required to extrude the paste from the nozzle. This was done in order to investigate the pastes viscosity in similar conditions to those during printing. The paste was prepared and put into the same syringe and nozzle used in the printing. The loaded syringe was put in the Instron and the desired speed of the jog was set. The chosen speeds were: 5, 7, 10, 20, 30, 40 and 50 mm/min. The speed of the jog remained constant and the force required to maintain that speed was continuously logged. 3 replicas were done to obtain a representative average. The same 3 cartridges were used during the measurements in the same order to reduce error. The setup can be seen in figure 19. Before the paste was measured, the force required to push the empty syringe was measured so that it could be subtracted. The paste needed to be extruded in the absence of air bubbles or pockets. If present, they appeared as drops in the force required. If a lump was present it would be read as a spike. An example of the generated results can be seen in figure 20.

A range where the required force was steady was chosen and from the raw data the average force was determined. The force required for the respective syringe for the same range was subtracted. The average force of the 3 specimens was then determined. This was repeated for all the different speeds and thus using *eq. 13* and *15*, the shear rate and shear stress could be calculated.

In order to calculate the actual pressure-drop, more information was required. The method currently developed to measure the viscosity using printing cartridges and nozzles for high viscous pastes requires further development to be able to fully determine the pressure drop. One way to accomplish this is could be the Bagley end correction for capillary flow by using several nozzles of different lengths or by only using one longer ($L/R > 30$) and one measurement without nozzle. Implementing a way to measure the pressure at the nozzle tip would also be viable.

In order to create an estimated pressure drop, the viscosity measured in the rheometer at the corresponding flow rate at the nozzle tip was used to calculate the Reynolds number. Then the Darcy friction factor could be estimated by the Moody diagram and thus using *eq. 14* the pressure drop could be estimated. Several assumptions were done during the estimation, as that the tube was cylindrical and not cone shaped, as the paste behaved Newtonian and thus that the viscosity was constant regardless of the experienced shear rate.

The shear rate could be plotted against the shear stress for the different extrusion speeds and with *eq. 12* the viscosity was determined for the different pastes.



Figure 19 The Instron with a loaded syringe.

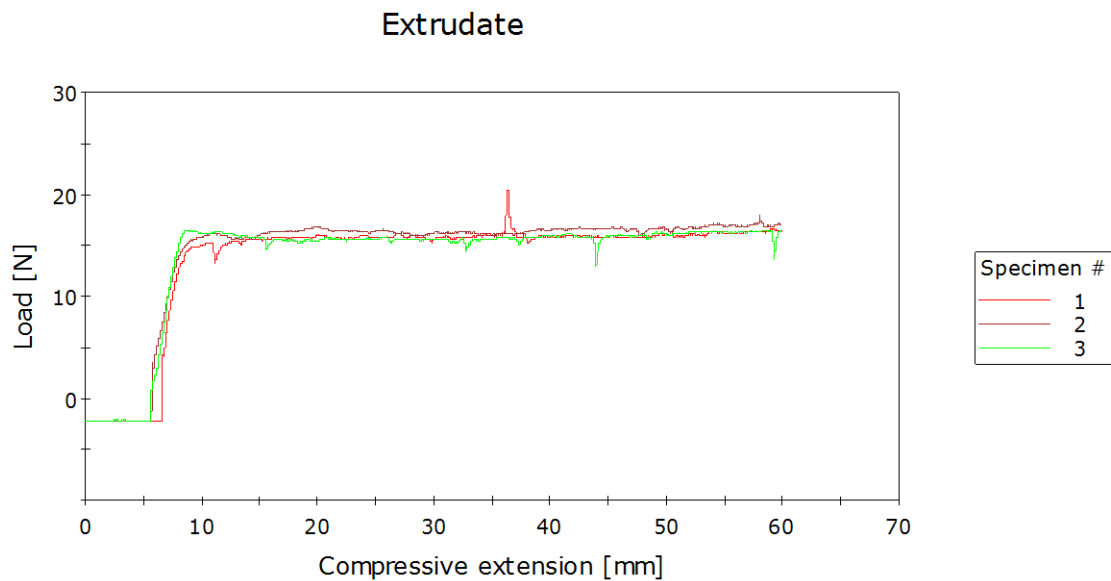


Figure 20 Example of the result generated by the Instron.

5.8.3 Particle size measurement

The particle size distribution of the different pastes and powders were measured with the Mastersizer 3000 (Malvern Pananalytical) which measures light scattering in order to determine the sizes and amounts of particles in a sample. The Hydro unit was used to analyse the pastes and the Aero unit to analyse the powders. For the Hydro unit, a small amount of the sample is dissolved in water and for the Aero unit the particles are suspended by a low pressure, whereupon the Mastersizer 3000 will provide the particle size distribution.

The Mastersizer 3000 requires the refractive index of the sample being measured. Since meat was not available in the database, cellulose was used since it was deemed the most similar material in the database. The settings for cellulose was a refractive index of 1.4683, an absorption index of 0.01 and a density of 1 g/cm³.

For the Aero unit, the loader gap was set to 2 mm, the air pressure to 2 bar, the feed rate varied between 50 and 70%, the number of measurements to 3 and all samples was run with 5 repetitions. The average was then determined.

For the Hydro unit, the stirring rate was set to 2000 rpm, the number of measurements to 3 and all samples was run with 5 repetitions. The average was then determined.

5.8.4 Structure

In order to get a better understanding the structures of the materials investigated and to verify the results from the Mastersizer 3000 a digital microscope with the option to magnify up to 1000 times was used to photograph both the powders and the pastes.

5.8.5 Printing

The figure chosen to compare the prints was one called “Gecko”, this due to the figure’s complexity, height and detail. The nozzle used had an opening with a 1.6 mm diameter and the speed was set to 100%, which was equivalent to 0.48 mm/min or 1.83 cm³ (paste)/min. All prints were done in room temperature on tiles.

5.9 COMPARISONS

5.9.1 Comparing: Amount of Thickener

In order to establish the characteristics of a printable paste, the concentration of thickener in the pastes was compared. 2 pastes with higher and 2 with lower concentrations of thickener than chosen formulation (25) (see Results and Discussion, Results Screening Trails, Screening Trails: Paste Formulation) was run through the set program in the rheometer to illustrate the rheological properties of printable pastes. They were also all used to print the “Gecko” figure in the 3D-printer. The concentrations tested were (in mM and weight percent thickener to water):

- 0.018mM, 3.5% xanthan gum.
- 0.013mM, 2.5% xanthan gum.
- 0.010mM, 2% xanthan gum.
- 0.008mM, 1.5% xanthan gum.
- 0.005mM, 0.5% xanthan gum.

5.9.2 Comparing: Takayanagi and Different Thickeners

To see if the paste could be separated into a xanthan and water phase and one protein and water phase, the paste was run in a centrifuge for 1 hour at 12 000 rpm. No separation occurred, so an approximation was made regarding how much the addition of the meat powder in the chosen formulation increased the thickening agent’s concentration to the water. The water with the appropriate weight percent of thickening agent underwent the same measuring program as the pastes in the rheometer to determine the meat powders effect of the xanthan system. 2 pastes mixed using sodium alginate was also investigated to further display the behaviour of nonprintable pastes with too low viscosity. The investigated solutions were (in mM and weight percent thickener to water):

- 138.9mM, 3% xanthan gum.
- 23.1mM, 0.5% sodium alginate (1:2.5 meat to water ratio).
- 23.1mM, 0.5% sodium alginate (1:3.3 meat to water ratio).

5.9.3 Comparing: Particle Size Using Different Milling

The particle size needs to be relatively fine when printing, thus the meat powder produced using different milling methods were analysed in the Mastersizer 3000s aero unit. The powers analysed were milled using:

- GM200 rotating blade food processor from Retsch for 5 seconds at 10 000, shaken and then repeated twice.
- GM200 rotating blade food processor from Retsch for 5 seconds at 10 000, shaken and then repeated twice followed by the ball mill MM301 from RETSCH at 25 Hz for 15 seconds.
- GM200 rotating blade food processor from Retsch for 5 seconds at 10 000 followed by the rotor mill from the company Fritch (the standard milling procedure used in the formulations).

5.9.4 Comparing: Particle Size Using Less Milling

The rotor mill from Fritsch were grinding everything extremely fine regardless it seemed of the material, and a quicker milling of the differently dried meats were investigated that would be easier to implement on a larger scale. The meat was grinded using the GM200 rotating blade food processor from Retsch for 5 seconds at 10 000, shaken and then repeated once. The powders were then analysed using the Mastersizer 3000s aero unit and compared using the digital microscope. The meat powders were dried using:

- 40°C without ultrasound.
- 40 °C with ultrasound.
- -15°C without ultrasound.
- -15°C with 50% power ultrasound.

To investigate if the higher moisture content in the hot air-dried meat reduced the friction enough during the milling to affect the size reduction, the moisture content was lowered to closer mimic the cold air-dried samples by placing samples in a fan forced oven at 85°C for 15 min. The moisture content after can be seen in table 4.

Table 4: Moisture contents of the differently dried meats samples after further drying.

Drying Method	Moisture content (average of the 2 samples)
Hot air without ultrasound	5.92 weight%
Hot air with ultrasound	7.19 weight%

5.9.5 Comparing: Dry and Wet Particles

To investigate if and how much the meat particles swelled in water, the following samples were analysed using the Mastersizer 3000 (the powder using the Aero unit and the wet samples using the Hydro unit) and looked at with the digital microscope:

- Powder produced by the standard milling procedure.
- Powder produced by the standard milling procedure with water carefully added.
- Paste produced by the standard procedure.

5.9.6 Comparing: Drying Method

Once the type and concentration of additive was chosen in combination with the meat to water ratio, the same procedure could be utilized to prepare paste of meat that had been dried using different methods, thus investigating the dryings impact on the printability. All pastes were measured in the determined program in the Instron, the particle sizes of the pastes were investigated in the Mastersizer 3000s Hydro unit, the rheological behaviour was determined by the set program in the rheometer, the structure was looked at with the digital microscope and they were all used to print the “Gecko” figure in the 3D-printer.

4 pastes produced using the same method and formulation was produced, containing meat dried using:

- 40°C, without ultrasound.
- 40°C with ultrasound.
- -15°C without ultrasound.
- -15°C with 50% power ultrasound.

6 RESULTS AND DISCUSSION

6.1 DRYING KINETICS

6.1.1 Hot air kinetics

As can be seen in figure 21, the meat being dried with the added ultrasound dried quicker. It is also notable that the samples -US1 dried quicker than -US2 and +US1 dried quicker than +US2. This was assumed to be because those samples were placed closer to the hot air inlet in the oven, thus experiencing a higher degree of forced convection. To compensate for this, an average of the 2 samples with and without ultrasound was calculated and can be seen in figure 22. The samples with ultrasonic assisted drying were calculated to get dry 40% faster which could be determined to be only due to the addition of ultrasound.

As can be seen in figure 23, the temperatures inside of the meat samples and the air temperature around the sample are plotted together with the drying rate. It can be seen that temperature inside and around the samples are equal. It can thus be argued that the increase in drying rate is only caused by the addition of ultrasound and not by additional heating from either the transducer or friction caused by the vibration inside of the sample. In both samples the inner temperature goes up when almost no moisture is remaining. This was assumed to be due to lack of any further moisture to evaporate, in other words when there was water present excess energy was used by the evaporation enthalpy to evaporate the water.

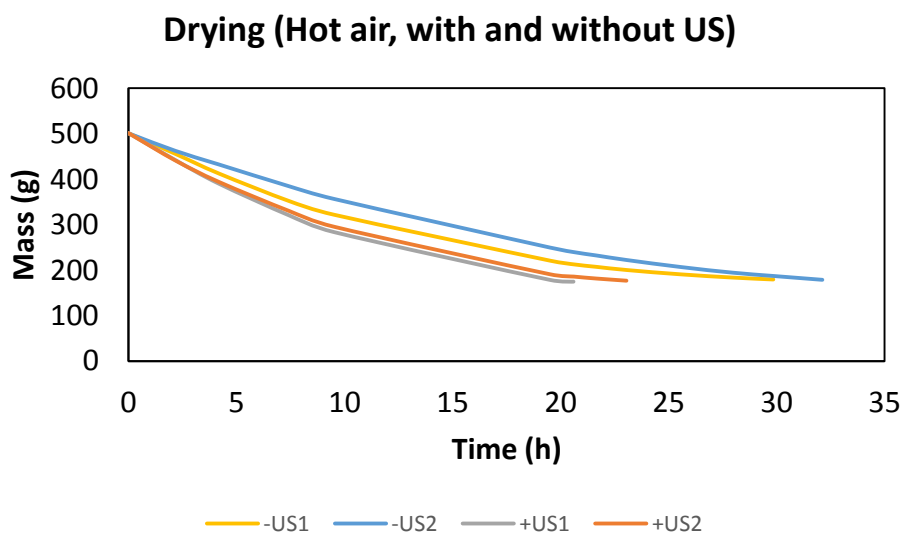


Figure 21 Drying speed of hot air-drying. (+US) stands for “with ultrasound”, (-US) stands for “without ultrasound”. The numbers stand for each of the 2 replicas.

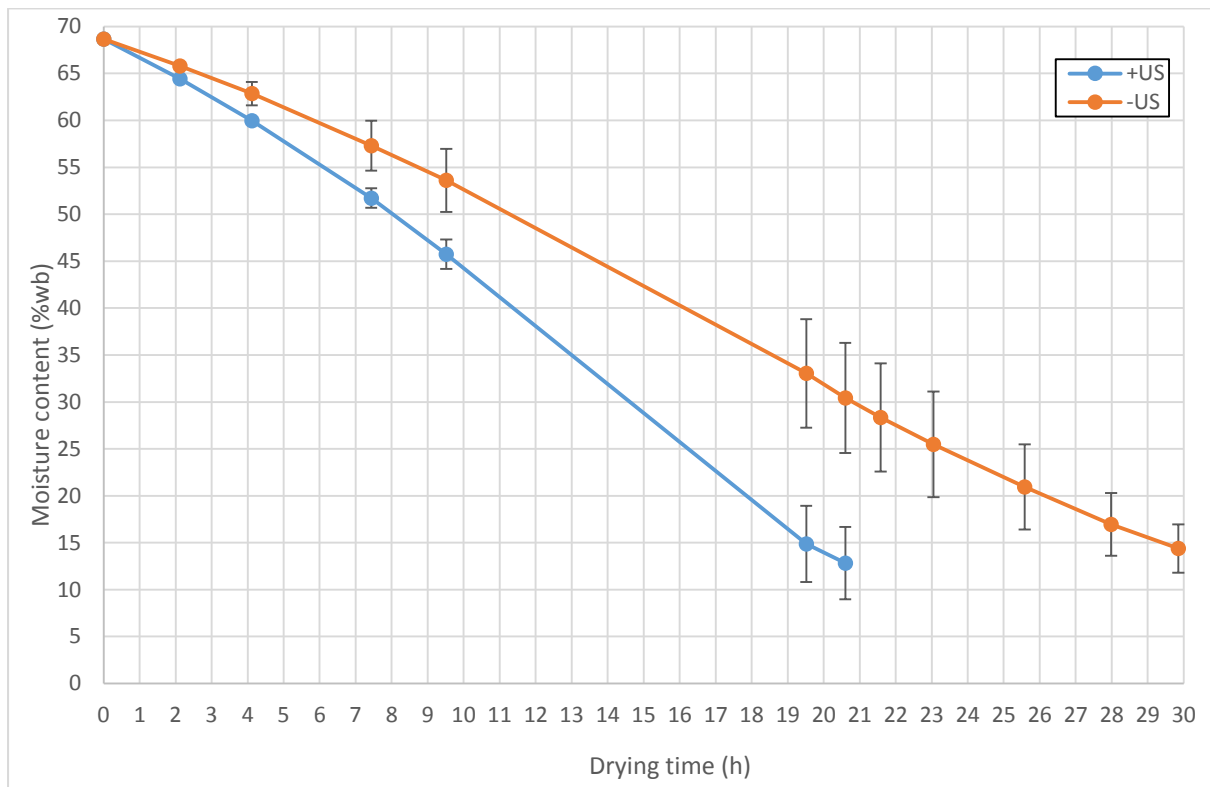


Figure 22 Drying speed of hot air-drying. (+US) stands for "with ultrasound", (-US) stands for "without ultrasound".

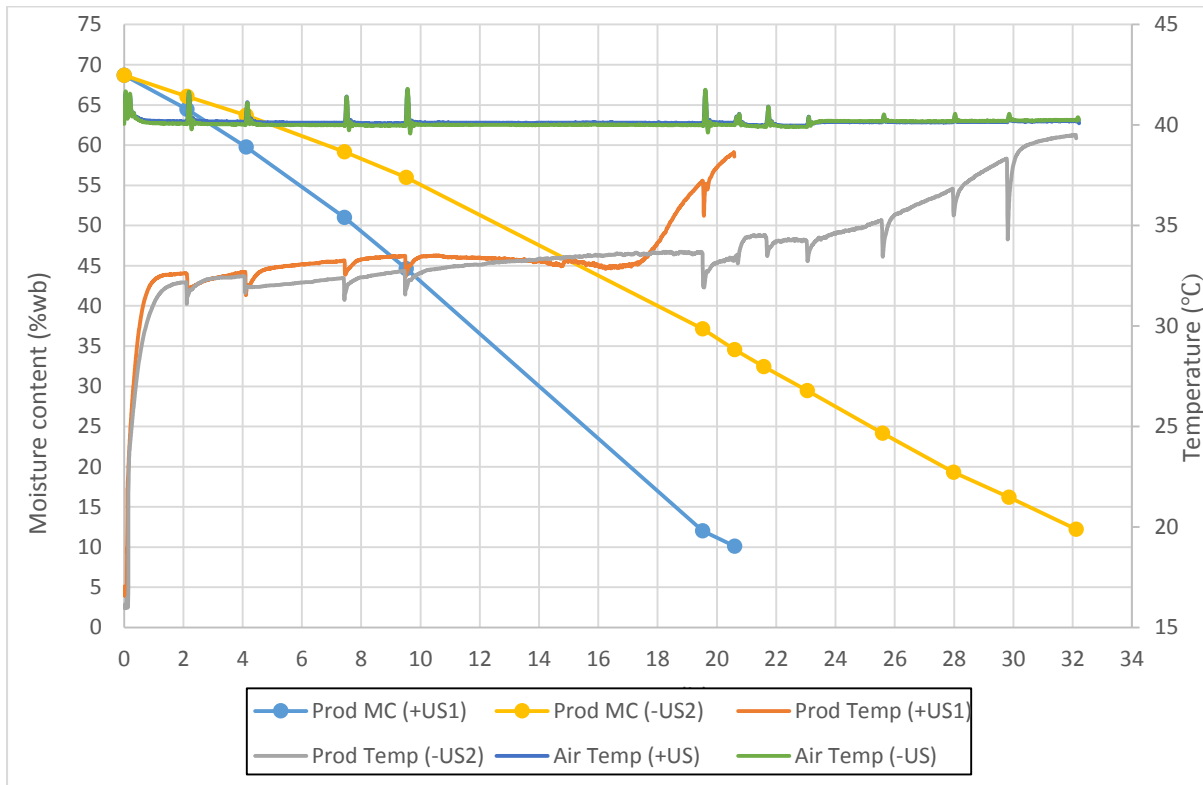


Figure 23 rod MC stands for product moisture content, Prod Temp stands for product temperature, Air Temp the air temperature near the product, -US stands for without ultrasound and +US stands for dried using ultrasound.

6.1.2 Atmospheric freeze-drying kinetics

As can be seen in figure 24, the meat being dried with the added ultrasound dried substantially more rapidly. The drying speed decreases as the driving force, or the concentration of water, decreases in the sample. For the sample being dried with ultrasound, it almost reached an equilibrium. Increasing the power of the ultrasound made the sample reach an equilibrium at a lower concentration of water, but this might have been affected by the temperature of the ultrasonic transducer increasing.

As can be seen in figure 25, the temperature of the sample placed on the ultrasonic transducer can be seen to have a higher temperature than the other. The transducer had a flow of cooling agent flowing underneath the surface, but it was assumed that at the pump was not strong enough to pump a sufficient amount of agent to cool the transducer to the desired temperature of -15°C . The sample temperature was measured to be above freezing temperature for a long duration of the drying, though no melting was observed, and the samples appeared identical. The higher measured temperature was estimated to be because the sensor was placed underneath the meat, thus coming in closer contact with the heating transducer. Since no melting occurred, then the meat that was probably cooled enough by the air to be at a temperature below freezing. If the increased temperature in the sample would have been due to friction caused by the ultrasonic vibration, the top layer should have caused melting of surrounding ice.

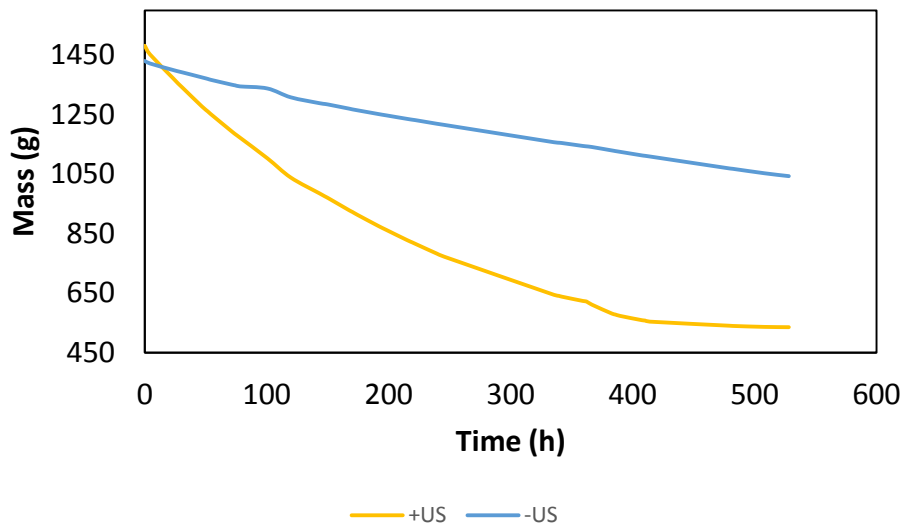


Figure 24 Drying speed of atmospheric freeze-drying. (+US) stands for “with ultrasound”, (-US) stands for “without ultrasound”. The power of the transducer was increased to 75% and a plastic conveyor belt was removed after 362 hours.

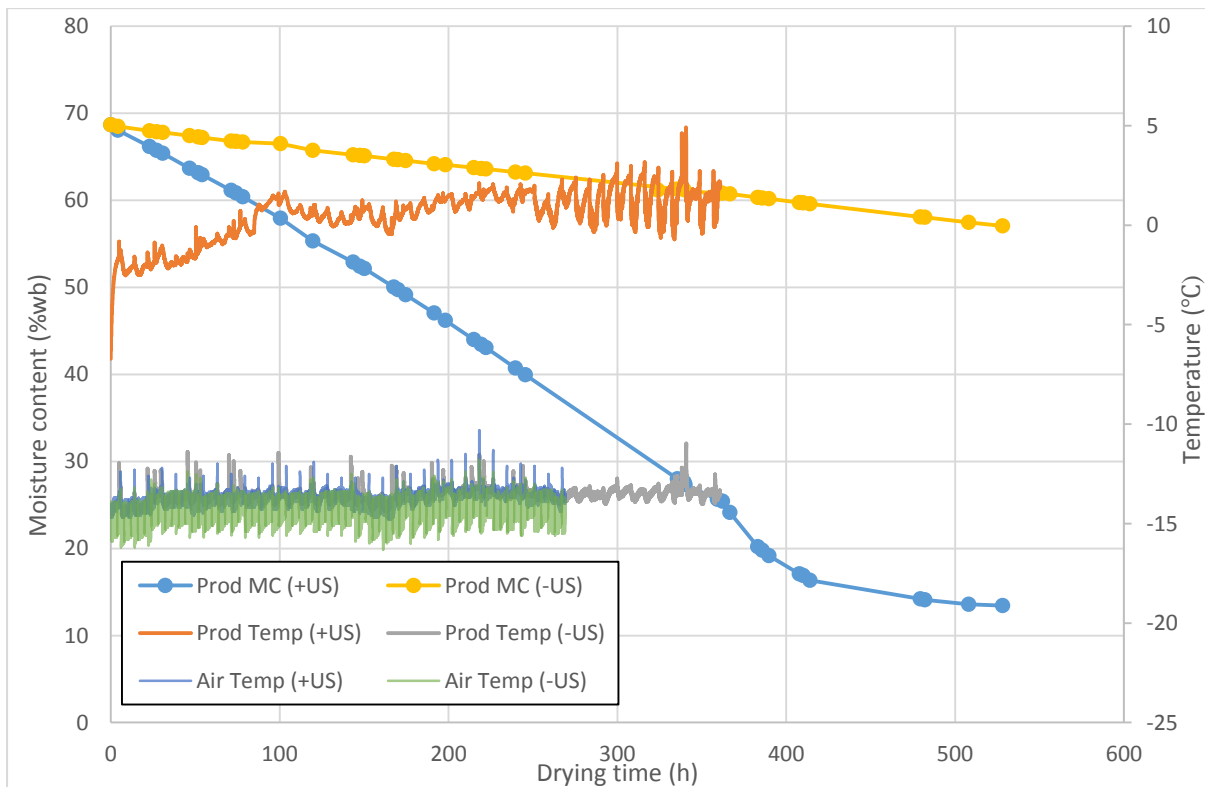


Figure 25 Prod MC stands for product moisture content, Prod Temp stands for product temperature, Air Temp the air temperature near the product, -US stands for without ultrasound and +US stands for dried using ultrasound.

6.2 LOSSES OF MEAT

During the pasteurisation and preparation for the drying on average 21.4% of the weight, excluding moisture, was lost.

It was calculated that during the standard milling procedure on average approximately 10% of the total weight of the dried meat in mass was lost.

6.3 DRIED MEAT

During the milling it became clear that lower concentration of lipids and water greatly facilitated the milling. Too high concentration of lipids and moisture caused the particles to stick together and to the surfaces of the different mills, thus hindering the size reduction. The reduction of the particle size is crucial for both the rehydration of the meat and to enable easy flow through the nozzle of the printer to minimize shooting. While there was no apparent difference by manual inspection between meat dried using ultrasound or not, there were a clear difference between the meats dried using hot or cold air, which can be seen in figure 26. The meat dried in a cool temperature had a brighter colour, was lighter and porous enough to almost be pulverized by hand. The meat dried using the hotter air was darker, denser, more solid and contained many very hard large particles. The rotor mill from Fritsch is very powerful and after its usage, the difference of the meat samples was greatly reduced to the point that they could not be told apart, which can be seen in figure 27.

Magnified pictures of the differently dried meats can be seen in figure 28. While no apparent difference was identified with or without ultrasound, looking more closely at the coldly dried air meats the porosity becomes apparent in comparison with the hot air-dried meats where the pores are closed, making it more solid. Magnified pictures of the corresponding powders can be seen in figure 29. No real difference was spotted. All the samples contained a small fraction of darker particles that was assumed to be burnt particles from the rotor mill.



Figure 26 Differently dried meats. Top left: cold air without US, top right: cold air with US (50% power), bottom left: hot air without US and bottom right: hot air with US.



Figure 27 Differently dried meats milled using the standard milling procedure. Top left: cold air without US, top right: cold air with US (50% power), bottom left: hot air without US and bottom right: hot air with US.

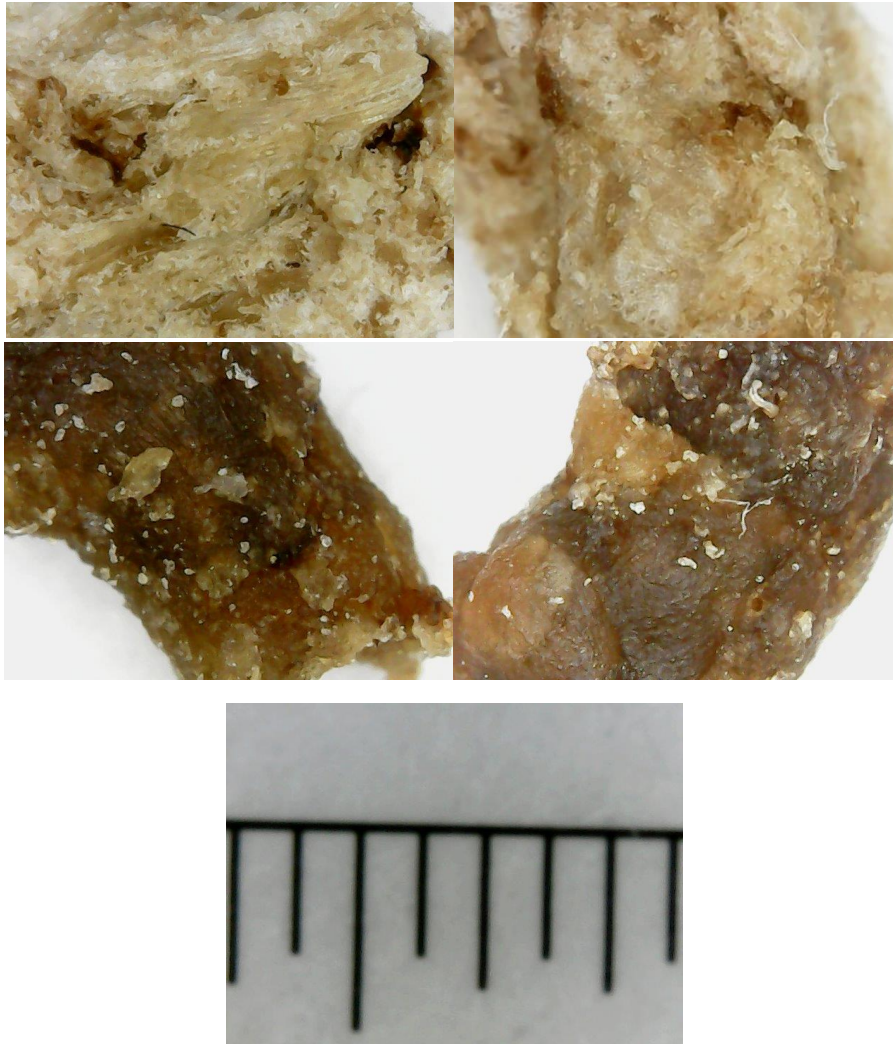


Figure 28 Differently dried meats. Top left: cold air without US, top right: cold air with US (50% power), bottom left: hot air without US, bottom right: hot air with US and bottom: ruler, every gap represents 0.5mm

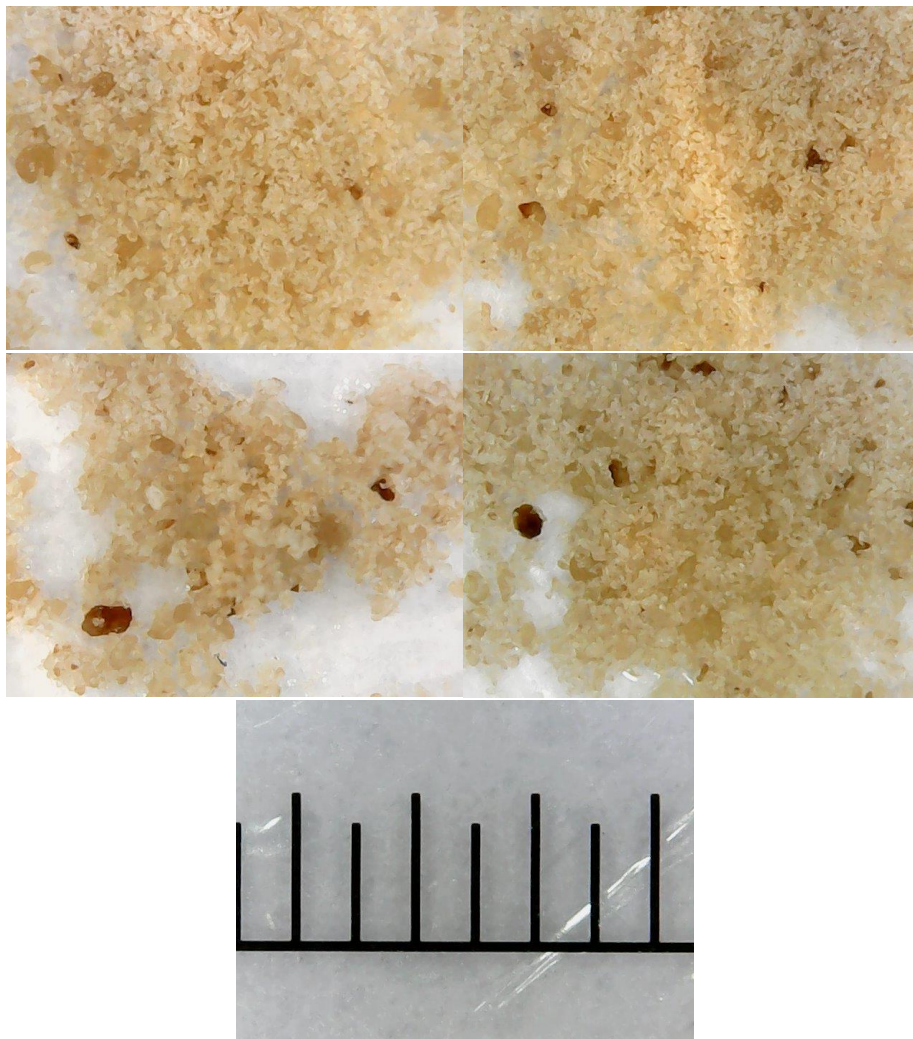


Figure 29 Differently dried meats, milled using the standard milling procedure. Top left: cold air without US, top right: cold air with US (50% power), bottom left: hot air without US, bottom right: hot air with US and bottom: ruler, every gap represents 0.5mm.

6.4 RESULTS SCREENING TRIALS

6.4.1 Screening Trials: Paste Formulation

The results from the screening trial can be seen in tables 5 and 6. Different characteristics of the printed figures was chosen to represent the printability of the formulations. The numerical value as assigned to the print's qualities were 1 was "low" and 5 "high". The chosen optimum formulations were (20) using the sodium alginate and (25) using the xanthan gum.

Table 5: Physical appearance of pastes by optical examination of sodium alginate paste.

Sample name	Thick- Ness*	Flow by gravity*	Breakage	Shooting	Print detail *	Visible printed lines *	Print hold *	Note for future trails
(3)	2	5	No	No	1	1	1	Higher viscosity and rigidity in figure needed.
(4)	4	3	Yes	No	1	4	3	Lower viscosity and higher sheer thinning behaviour needed.
(7)	1	-	-	-	-	-	-	Unprintable, viscosity too low.
(8)	1	-	-	-	-	-	-	Unprintable, viscosity too low.
(9)	4	5	No	No	1	2	2	Paste too thick to properly print. Not "gel-like" enough, could not hold its structure. Better results at lower printing speeds. Paste became too firm after cooling, a lot of "breaking" occurred then.
(10)	4	4	Yes	No	2	2	2	Not "gel-like" enough to hold its structure. Better results at lower printing speeds. More able to sustain its shape after cooling, but still a lot of breaking.
(11)	5	-	-	-	-	-	-	Very dry paste, unprintable.
(12)	5	2	Yes	Yes	3	5	3	Very dry and too thick paste,

(13)	3	1	No	No	4	4	4	Held its structure. Less visible lines in finished figure at lower printing speeds.
(20)	3	1	No	No	5	4	5	Held its structure well. A bit gel-like when attempts on moving the figure was done.
(21)	5	1	No	Yes	5	4	5	Too thick. Could be picked up after cooling.
(23)	3	1	No	No	5	4	5	Held its structure well. Could almost be scraped up after printing. Could be picked up after cooling.

*1 = Low, 5 = High

Table 6: Physical appearance of pastes by optical examination of xanthan gum paste.

Sample name	Thick- Ness*	Flow by gravity*	Breakage	Shooting	Print detail *	Visible printed lines *	Print hold *	Note for future trials
(15)	2	5	No	No	2	2	2	To low viscosity. Could not hold its structure. Looked like it melted.
(16)	2	3	No	No	2	2	2	To low viscosity. Could not hold its structure. Looked like it melted.
(17)	2	3	No	Yes	3	2	3	To low viscosity. Could not hold its structure.
(18)	2	3	No	No	3	3	3	Could almost hold its structure. Could not be moved, viscosity too low.
(19)	2	2	No	No	5	3	4	Held its structure well. Could not be moved, viscosity too low.
(24)	3	2	No	Yes	4	3	4	Held its structure well. Could not be moved, viscosity too low.
(25)	3	1	No	No	5	4	5	Held its structure well. Could not be moved, viscosity too low.
(28)	4	1	Yes	No	5	5	5	A bit of dragging occurred. The high xanthan gum concentration made the paste "rubbery".

*1 = Low, 5 = High

An additional investigation on whether the mix of xanthan gum and gellan gum would provide more favourable rheological properties was conducted. There was a slight increase in viscosity, but the formulation only using xanthan gum was favoured.

The trial showed that pastes with higher concentrations of thickeners and meat powder resulted in a yield stress that made the cartridges harder to fill due to its reluctance to flow into the empty pockets, thus creating bubbles. Bubbles in the cartridge will result in missing parts of the finished printed figure.

Using the 3D printers built in heater during printing of the "Gecko" shape did not prove successful. The maximum temperature of the plate was not hot enough to cook the figure, but only dry the bottom layer.

Once a figure is printed it starts to dry, thus losing its gloss and becoming firmer. Especially for the paste produced using sodium alginate, the figure becomes a lot firmer. This was drastically reduced though covering the printed figure as soon as the printing is complete. Keeping the print cold once covered maintains the pastes properties for a long time after printing.

A cooking process for the figures need more work to be perfected. In figure 30, figures prepared using formulation (25) can be seen that has been cooked for 10 minutes, at 180°C in a fan forced oven. A hard shell covered the figure, but the interior remained almost unaffected. Cooking proved difficult with a figure as the Gecko that contained thin layered parts that dried completely when heated.



Figure 30 Paste created using formulation (25), cooked for 10 minutes at 180°C.

6.4.2 Screening Trails: Optimum Thickener

Prints utilizing paste from either sodium alginate or xanthan gum could be printed into the desired figure when mixed in suitable concentrations. To compare meat pastes prepared using the different drying methods though, the xanthan gum was selected. This because despite the prints looked similar, which can be seen in figure 31, the paste prepared with xanthan gum proved to be easier to prepare and scale. This made it easier to handle and reduced uncertainties while the drying was to be compared.

Both the paste prepared using sodium alginate and xanthan gum can have commercial use. Sodium alginate is being investigated for instance for its dietary properties and provided a paste that after printing became rather solid, even more so after cooling. The figures created with xanthan gum had a stickier feel, even after cooling. This could be used for instance to provide food for people with difficulties swallowing, as people with dysphagia.

Both mixing xanthan gum and sodium alginate in the paste to print increased the viscosity and providing the paste a shear thinning behaviour that is greatly improving 3D printability, when added in the right amounts. Only creating a paste with shear thinning behaviour is not enough though. When creating a new paste for printing, work needs be done to formulate viable printing characteristics,

such as a yield stress and suitable amount of shear thinning since food vary severely in composition and characteristics. The work does though provide the impression that most foods can be printed if their particle size is reduced enough, proper rehydration occurs and an appropriate viscosity is achieved.

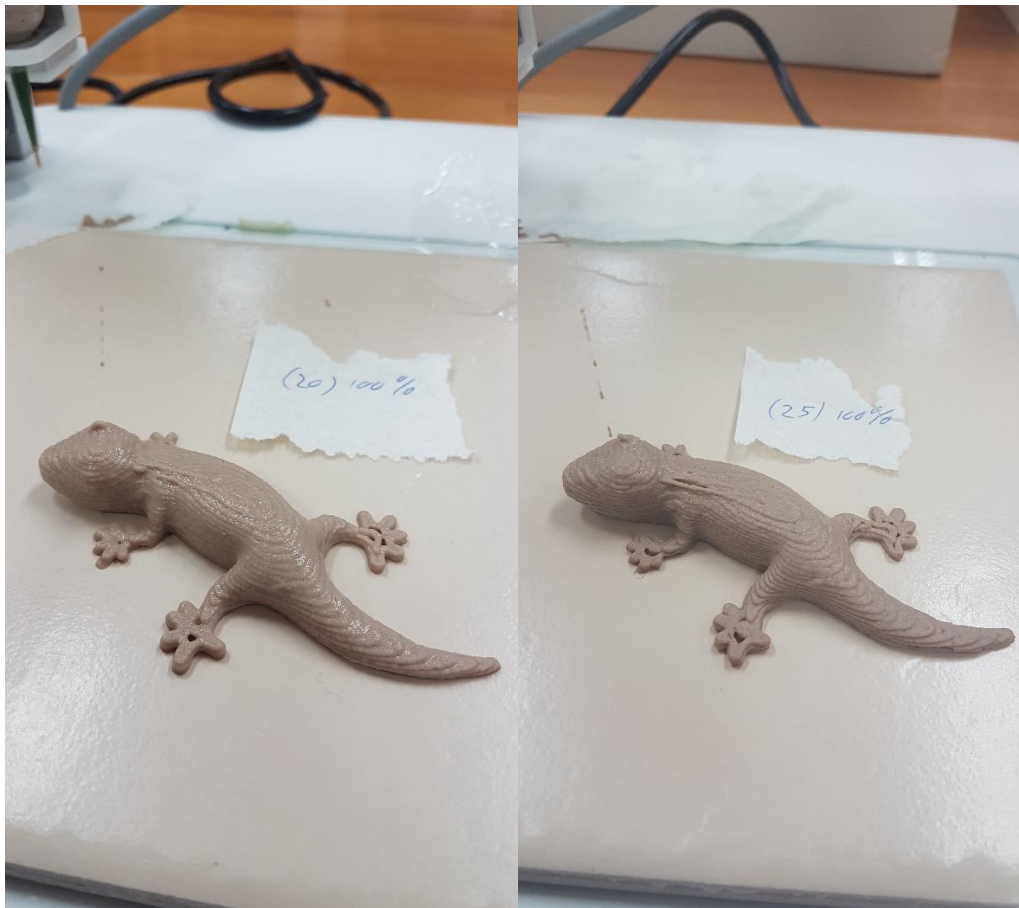


Figure 31 Printed pastes of formulation (20) (sodium alginate) to the left, and (25) (xanthan gum) to the right.

6.5 RESULTS: AMOUNT OF THICKENER

In figure 32, paste created using cold air-dried meat in 1:2.5 ratio to water with different concentrations of xanthan gum is investigated by the first rheometer program. Until shear rate of approximately 0.1/s it was assumed that cracking in the pastes, especially in the paste with higher concentrations of xanthan gum, caused the measured viscosity to be measured than anticipated. Within the range between 0.1/s to around 50/s the relation between increasing concentration of xanthan gum increased the viscosity at different shear rates can be observed. Over shear rates of 50/s it was assumed that the rotational speed of the vane was too high for the paste to flow back into the vane, thus the sudden drop in the measured viscosity.

Yield stress is an important factor in printing, in the pastes it was assumed that the yield stress followed the viscosity. The results of the second program can be seen in figure 33 and their printed

figures using the different pastes can be seen in figure 34. The figure with 0.005mM or 0.5% xanthan gum had a too low viscosity to be printed and the one with 0.008mM or 1.5% xanthan was prone to slumping. The viscosity thus needed be above 200 000Pa*s after printing for the figure to keep. The pastes with 0.010mM or 2% and 0.013mM or 2.5% xanthan gum proved viable for printing. The one with 0.018mM or 3.5% xanthan gum had a viscosity too high for proper printing, the printed lines need to flow a little in order to create a smooth figure. The viscosity of a paste should then not exceed 400 000Pa*s the first seconds after it has been printed. Thus, for a printable paste the viscosity just after printing should be between 200 000 to 400 000Pa*s, which using the presented method was achieved using 2 to 2.5 weight% to the water. This stands as an indicator of the proper and viable initial viscosity for a successful print.

Comparing the viscosity of the meat paste in regards of the shear rate was done in another study that aimed to print mashed potato with different concentrations of potato starch. They found similar correlation between viscosity and shear rate for printable paste [23].

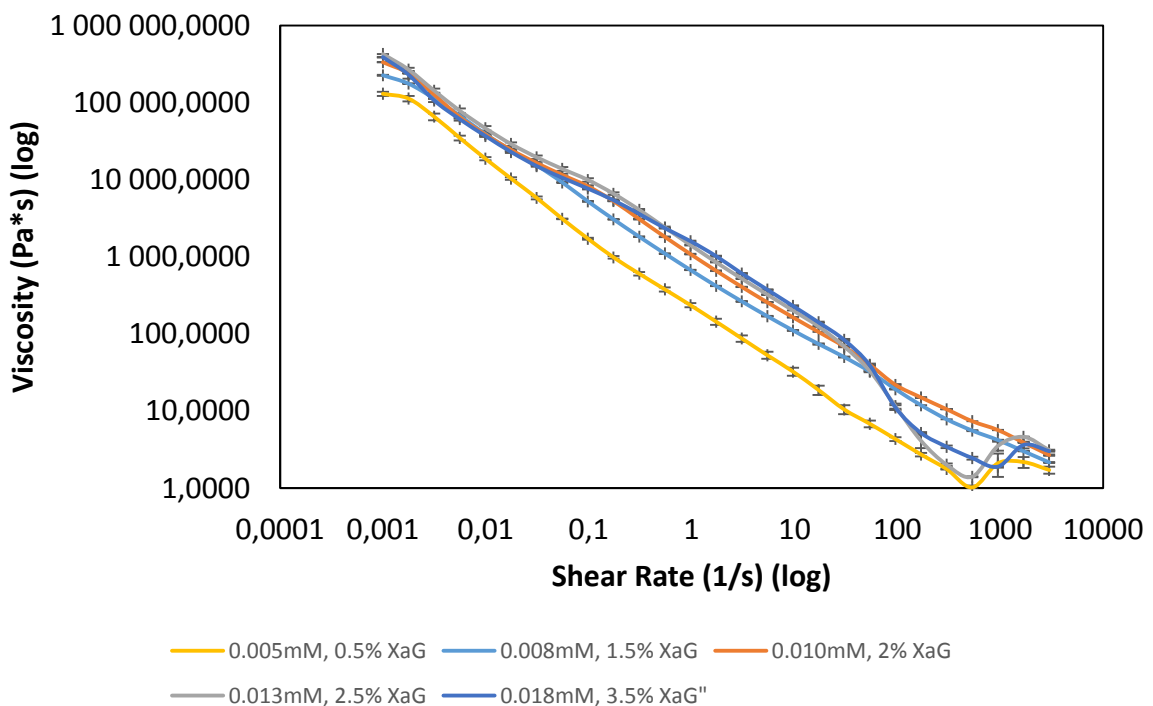


Figure 32 Apperent viscosity to shear rate of meat pastes formulated using different amounts of xanthan gum.

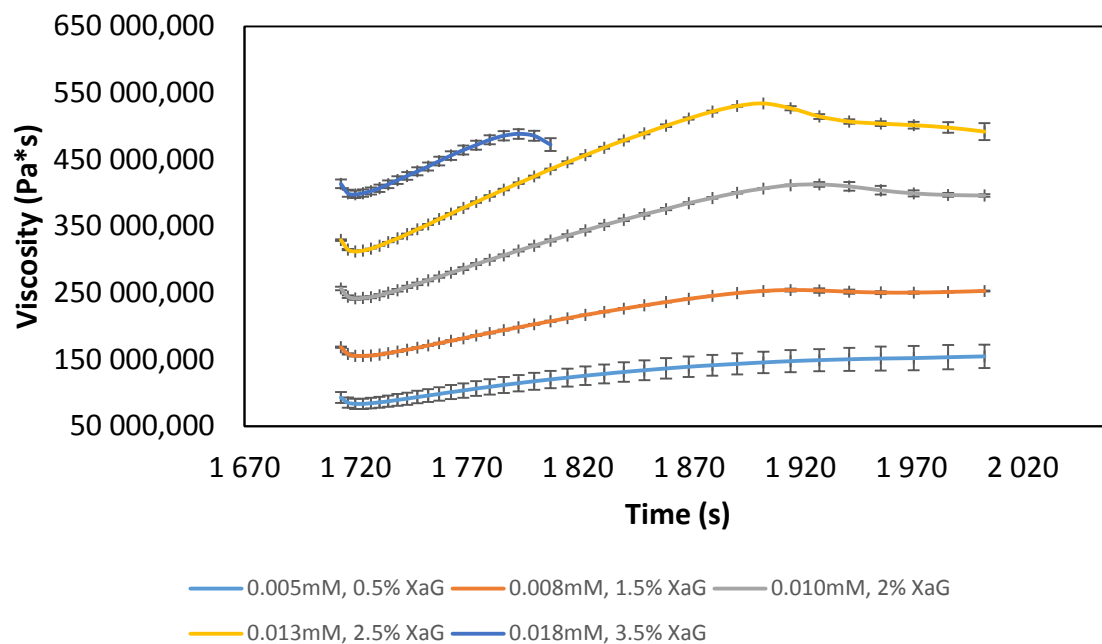


Figure 33 Apparent viscosity to time when suddenly decreasing the shear rate from 3000/s to 0.001/s of meat pastes formulated using different amounts of xanthan gum.



Figure 34 Figures to be compared to formulation (25). All containing 1:2.5 meat to water ratio. Top left: 0.5% xanthan gum, top right: 1.5% xanthan gum, bottom left 2.5% xanthan gum and bottom right xanthan gum. All weight% to water.

6.6 RESULTS TAKAYANAGI AND DIFFERENT THICKENERS

In figure 35 and 36, paste created using cold air dried meat in 1:2.5 and 1:3.3 ratio to water with 23.1mM or 0.5% xanthan gum together with water with 0.015mM or 3% xanthan gum in water is investigated by the first and second rheometer program respectively. The pastes provide information on the behaviour on past with too low viscosity to be printed. The xanthan gum in water in second program show that xanthan in water regains its viscosity rapidly, meaning that adding meat powder makes the paste regain its viscosity slower. While increasing the total viscosity of the mix, the added meat particles might obstruct and hinder in the formation of the rapid linkage of the xanthan molecules.

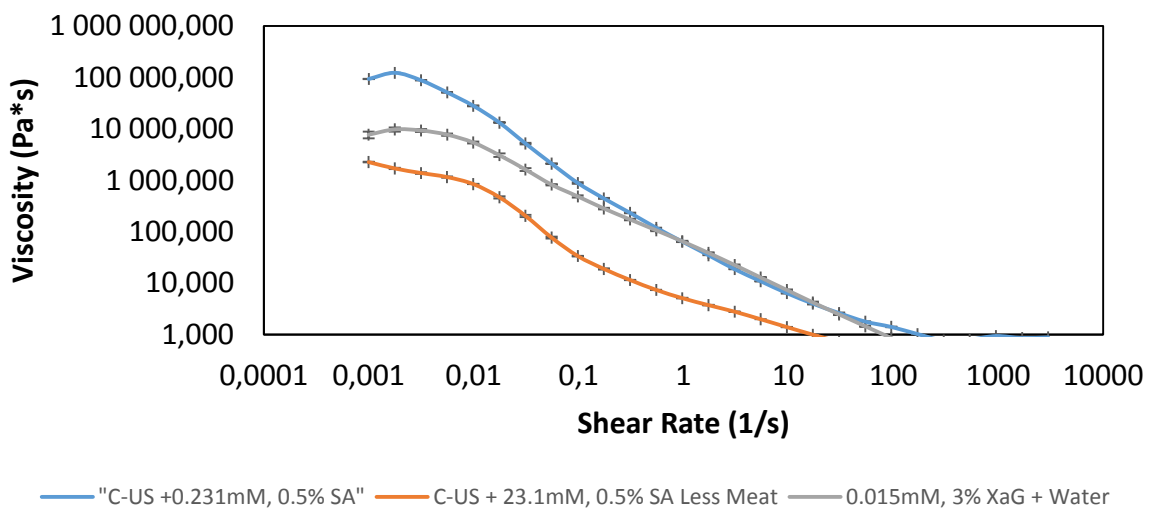


Figure 35 Change in viscosity to increasing shear rate. Cold air-dried meat 1:2.5 ratio with 23.1mM or 3 weight% to water xanthan gum, Cold air-dried meat 1:3.3 ratio with 23.1mM or 3 weight% to water xanthan gum and water with 138.9mM or 3 weight% to water xanthan gum.

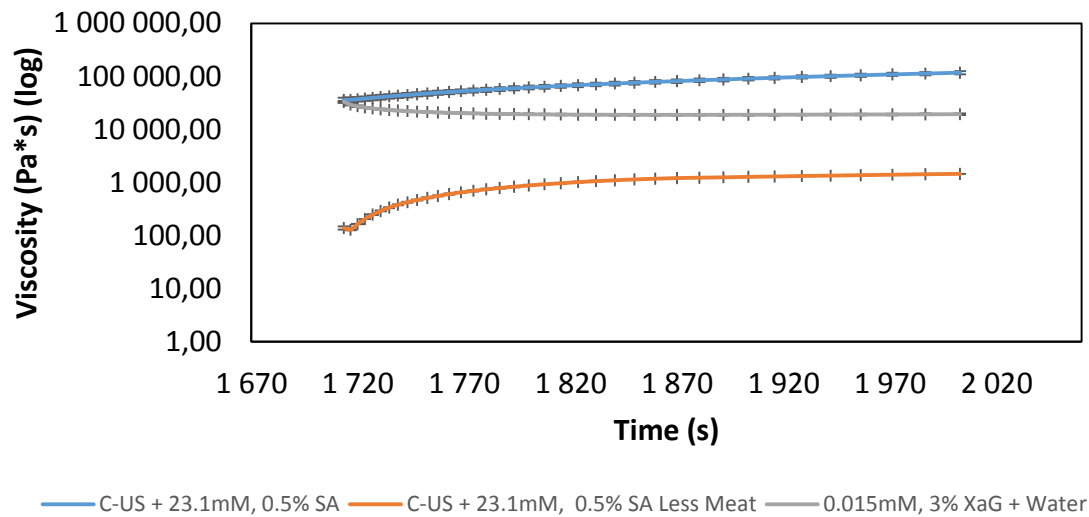


Figure 36 Change in viscosity over time. Sudden decrease in shear rate held constant. Cold air-dried meat 1:2.5 ratio with 23.1mM or 3 weight% to water xanthan gum, Cold air-dried meat 1:3.3 ratio with 23.1mM or 3 weight% to water xanthan gum and water with 138.99mM or 3 weight% to water xanthan gum.

6.7 RESULTS: PARTICLE SIZE USING DIFFERENT MILLING

For an efficient print the particle size is desired to be smaller than the nozzle size of the printer and generally smaller particles facilitate printing as it reduces shooting. The powders from the standard milling procedure was compared to powders using other methods. The other methods were:

- GM200 rotating blade food processor from Retsch for 5 seconds at 10 000, shaken and then repeated twice.
- GM200 rotating blade food processor from Retsch for 5 seconds at 10 000, shaken and then repeated twice followed by the ball mill MM301 from RETSCH at 25 Hz for 15 seconds.

The results from the Mastersizer 3000s Aero unit indicated that standard milling procedure produced the finest particles, followed by the rating blades and the ball mill, which can be seen in figure 37. The results are supported by investigating the powders in the digital microscope which can be seen in figure 38.

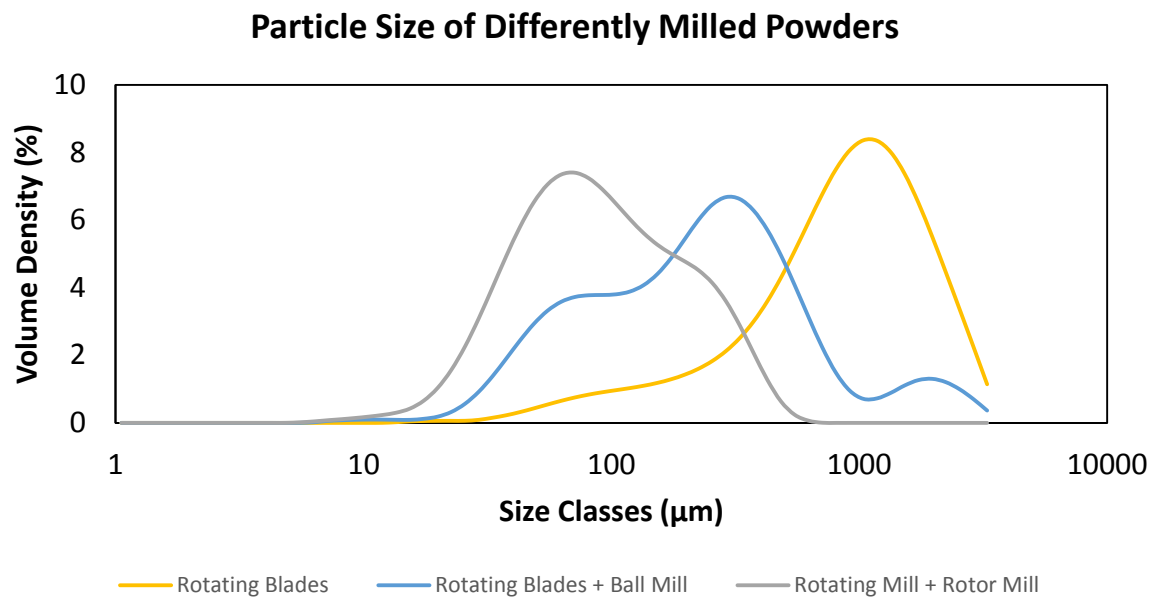


Figure 37 Particle size distribution of differently milled meat.

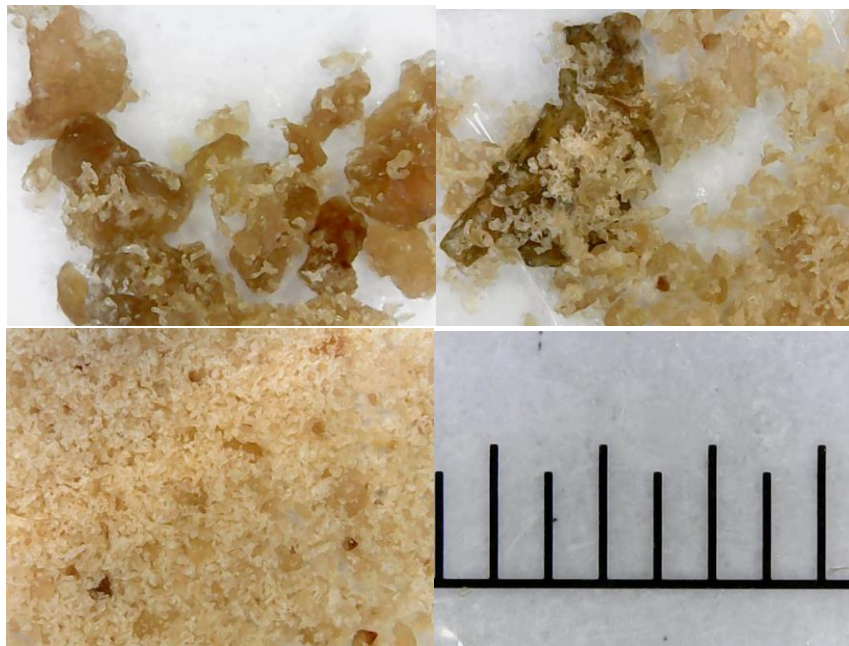


Figure 38 Dried meat using hot air with ultrasound, milled using: top left: GM200 (5 seconds * 3), top right: Gm200 (5 seconds * 3) + Ball Mill (25 Hz, 15 seconds), bottom left: GM200 (5 seconds) + Rotor mill and bottom right: ruler, every gap represents 0.5mm.

6.8 RESULTS: PARTICLE SIZE USING LESS MILLING

The four differently dried meats were all milled using the GM200 rotating blade food processor from Retsch for 5 seconds at 10 000, shaken and then repeated twice. The 4 powders were all analysed in Mastersizer 3000s Aero unit and the results can be seen in figure 39. The meat powders dried using cold air became a lot finer powder than the powders produced using hot air. The powder dried using cold temperature were porous and were pulverised when small amounts of force was applied. It could even be milled to a powder fine enough to print using only the GM200 rotating blade mill, this was not the case for the hot air-dried powder. The hot air-dried powder contained countless larger highly unyielding particles that were difficult break down while milling, these particles would make the paste a lot less printable both in term of solvability and causing shooting problems.

To investigate if the higher moisture content of the hot air-dried meat had an impact on the milling, this meat was dried further be better match the cold air-dried meat. As can be seen in figure 40, no significant difference was detected in the size reduction by lowering the moisture content to the same as the cold air-dried meat.

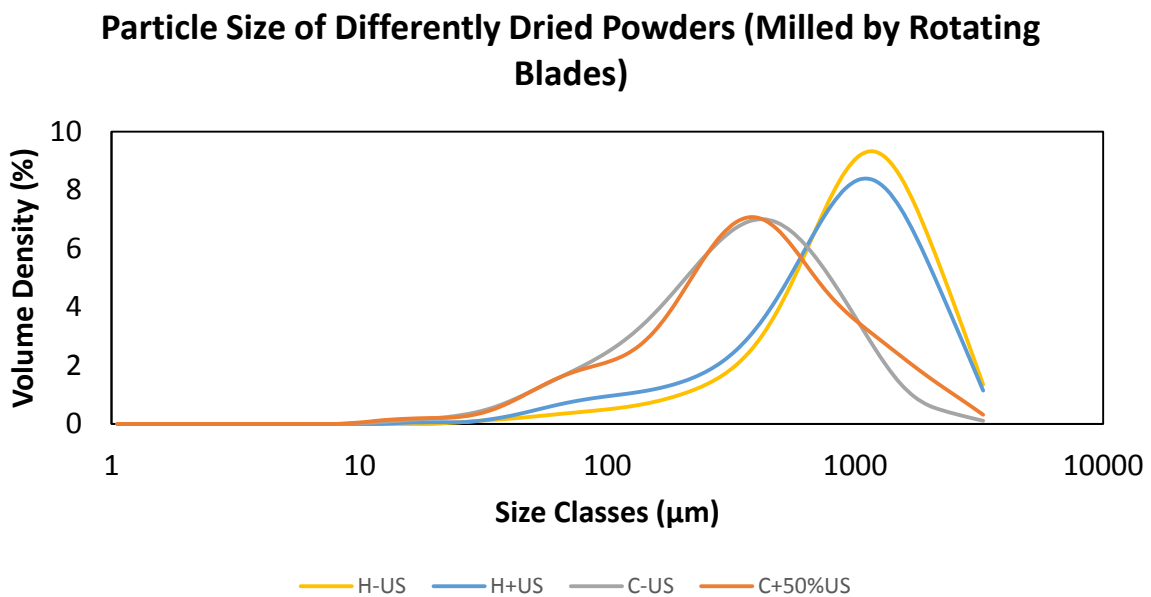


Figure 39 The particle size distribution of powders created by differently dried meats. H-US = hot air without ultrasound, H+US = hot air with ultrasound, C-US = cold air without ultrasound and C+50%US = cold air with 50% ultrasound power.

Particle Size of Hot Air Dried Powders with Different Moisture Content (Milled by Rotating Blades)

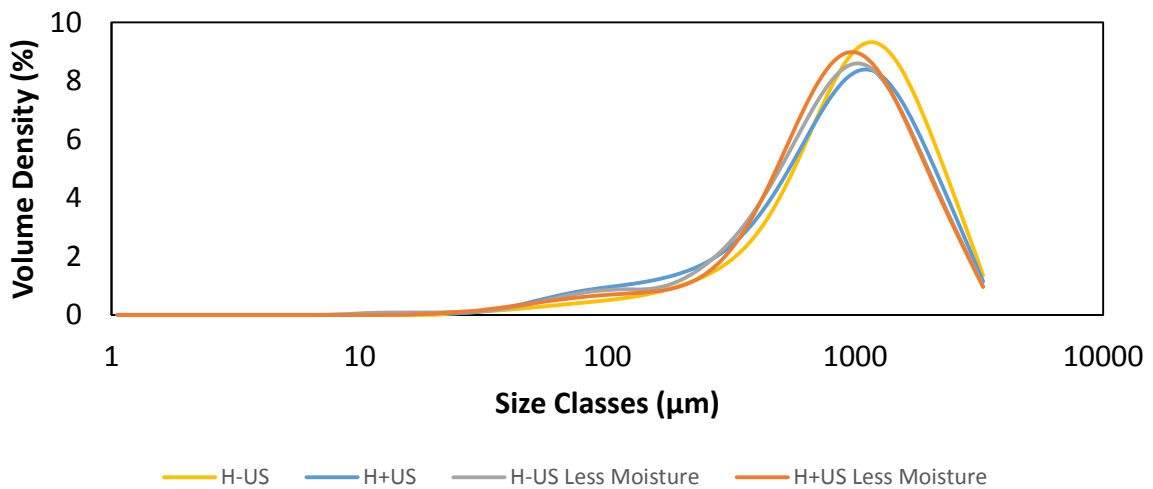


Figure 40 The particle size distribution of powders created by differently dried meats, compared with the same meats but drier. H-US = hot air without ultrasound, H+US = hot air with ultrasound.

6.9 RESULTS: DRY AND WET PARTICLES

Powders of the differently dried meats were analysed in the Mastersizer 3000s Aero unit, the same powder in water were measured in the Mastersizer 3000s Hydro unit and the same was done the finished pastes. The 3 versions of the different powders were compared to see if the particles were swelling in water, which can be seen in figure 41, 42, 43 and 44 and pictures of the comparison can be seen in figure 45 and 46. The powders in the water were generally smaller though, than when dry. This might be because of that during the measurement with the Aero unit, it looked like the particles were sticking together before they were measured, and more so for the cold air-dried particles. Thus, when dispersed in water, they dispersed from each other. It might also have been because some particles dissolved or due to differences in measurements between the Aero unit and the Hydro unit.

Some increase in particles size for the larger particles could be linked to swelling, this was recorded more for the hot air-dried powder though. In all cases the smallest particle size can be observed in the pastes. During the homogenizing the hand-held blender Stickmaster was used. Both the blender and the sieving evidently further reduced the average particle sizes of the pastes.

Replacing the handheld StickMaster with a stationary agitator run at 700 rpm was evaluated. This did not produce a homogenic enough paste, it had many larger particles which resulted in a lot of shooting during printing. The usage of the StickMaster thus provided proper homogenization and further reduction of the particles in the paste.

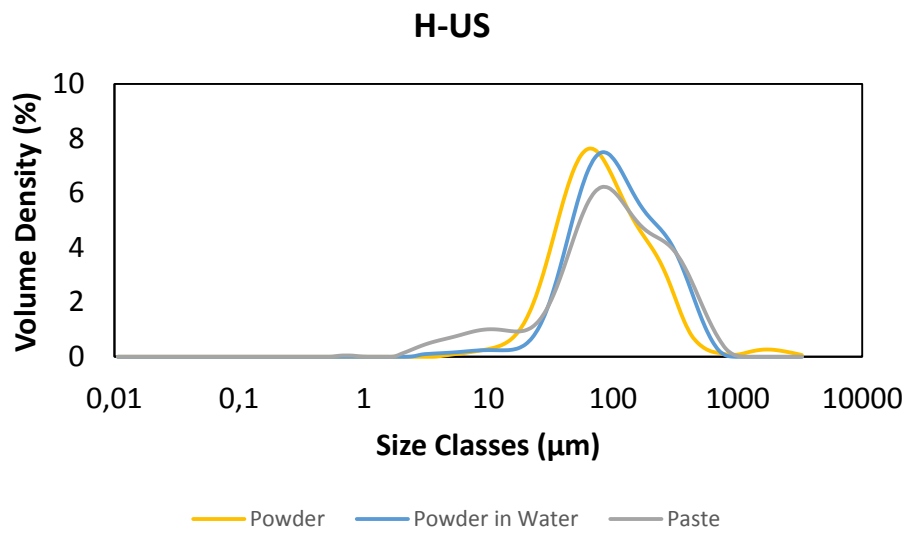


Figure 41 The size distribution of the powder, powder in water and the finished paste using hot air dried meat without ultrasound.

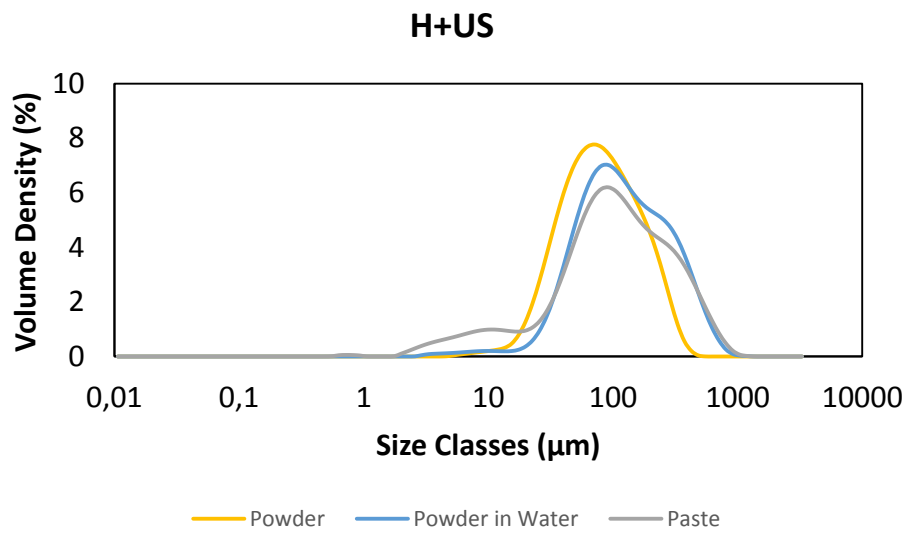


Figure 42 The size distribution of the powder, powder in water and the finished paste using hot air dried meat with ultrasound.

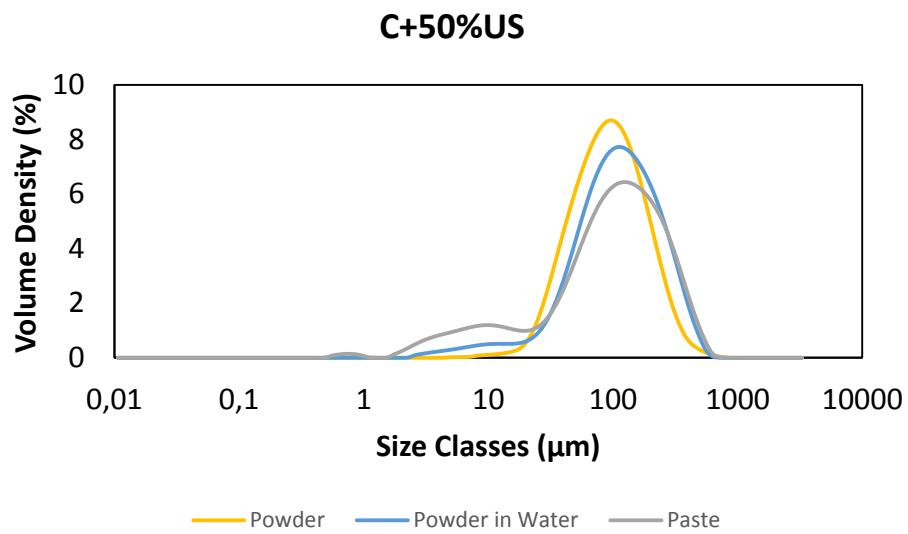


Figure 43 The size distribution of the powder, powder in water and the finished paste using cold air dried meat without ultrasound.

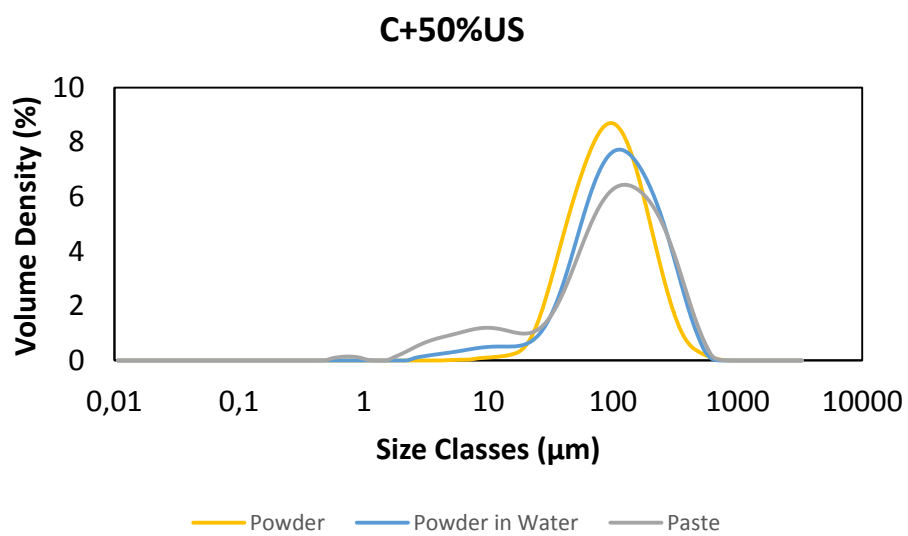


Figure 44 The size distribution of the powder, powder in water and the finished paste using hot air dried meat with 50% ultrasound power.

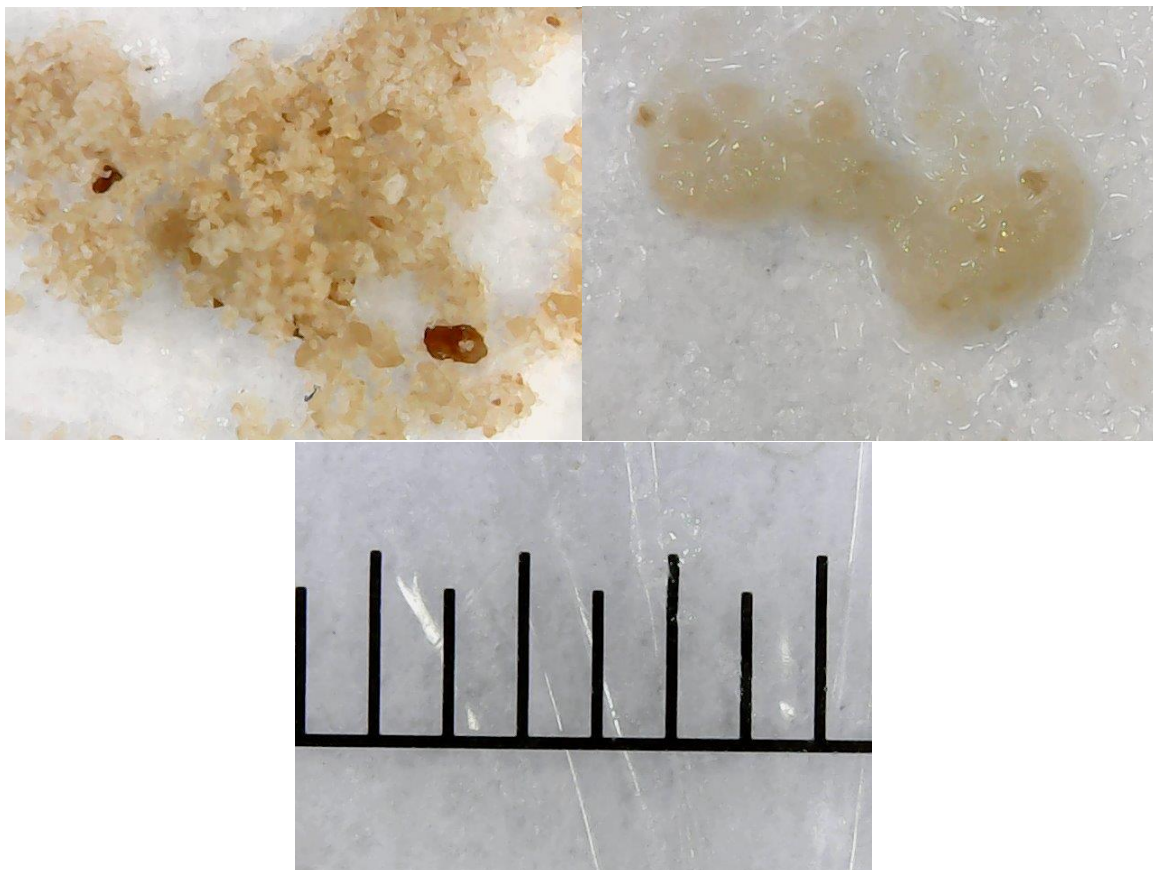


Figure 45 Meat dried using cold air without US. Top left: powder, top right: powder in water and bottom: ruler, every gap represents 0.5mm.

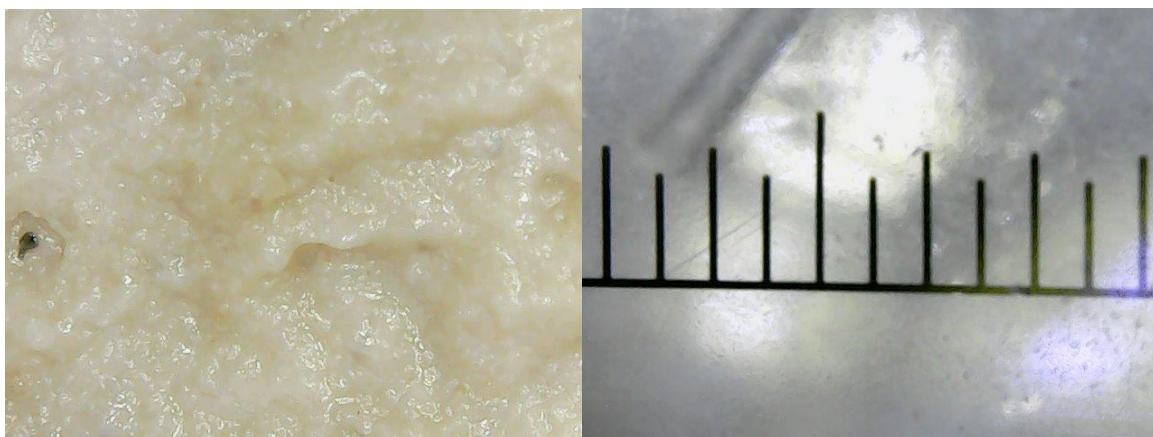


Figure 46 Meat dried using cold air without US. Left: paste and right: ruler, every gap represents 0.5mm.

6.10 RESULTS: DRYING METHOD

6.10.1 Drying Method: Rheology

The first program investigated the pastes behaviour when the shear rate increased. In figure 47. The pastes viscosity in correlation with the shear rate can be seen. All four behaved rather similar, the viscosity decreased as the shear rate increased. The 2 hot air-dried pastes had during the program slightly lower viscosity than the 2 cold air-dried pastes.

The second program was designed to look at how quickly the pastes regained their viscosity once the shear rate decreased, which is necessary in printing to more accurately control the print and to keep the figure from slumping. It is desired that the pastes viscosity rapidly increase after it has been extruded and that the paste has enough yield stress to maintain the following layers. The program was also to determine how high the final viscosity became. For the investigated pastes the time to settle is not relatively long, meaning that the time difference is not of a larger importance. It can also be assumed that viscosity will act as indicator on the yield stress, thus a paste with a higher final viscosity is favourable. The change in viscosity in correlation with the time passing can be seen in figure 48. Initially the viscosity drops slightly, this was thought be because of inertia from the end of the first program where the shear rate was high. The 2 pastes created using cold air-dried meat reached their final viscosity more rapidly, but the paste created using cold air reached a higher final viscosity, thus proving more favourable for printing purposes.

Possibly affecting the results of the rheological measurements of the paste would be slight differences in the formulation process or possible the minor difference in moisture content in the meat used in the formulations.

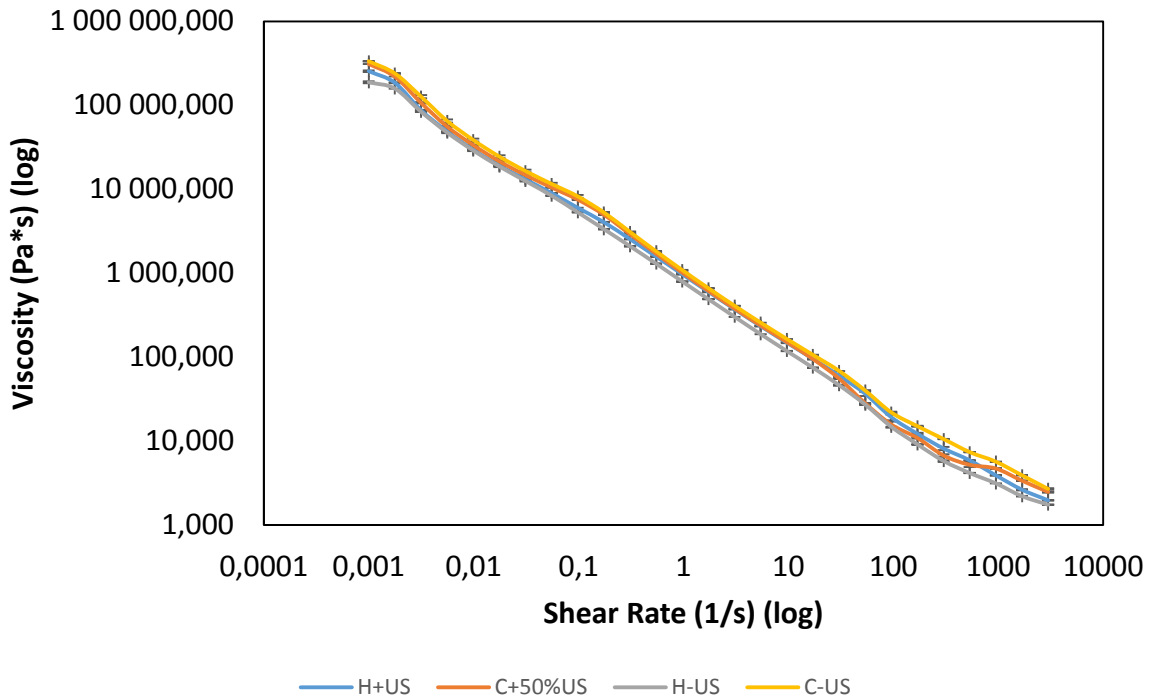


Figure 47 Apparent viscosity to shear rate of meat pastes formulated using differently dried meats. H-US = hot air without ultrasound, H+US = hot air with ultrasound, C-US = cold air without ultrasound and C+50%US = cold air with 50% ultrasound power.

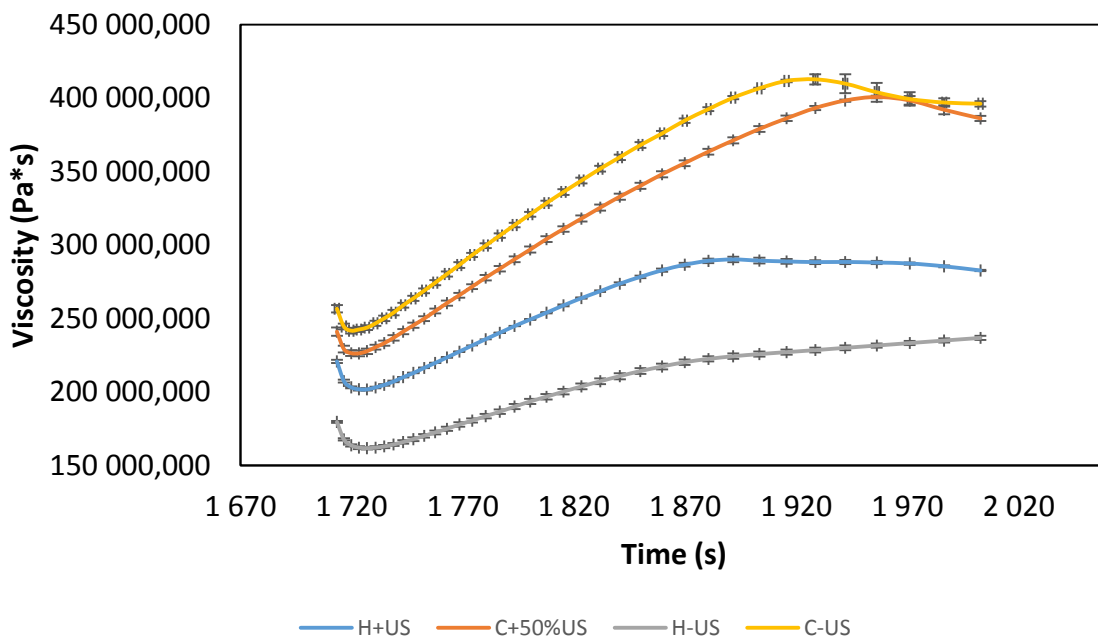


Figure 48 Apparent viscosity to time when suddenly decreasing the shear rate from 3000/s to 0.001/s of meat pastes formulated using differently dried meats. H-US = hot air without ultrasound, H+US = hot air with ultrasound, C-US = cold air without ultrasound and C+50%US = cold air with 50% ultrasound power.

6.10.2 Drying Method: Instron

The flow curves of the pastes created using the differently dried meat can be seen in figures 49, 50, 51 and 52. All 4 display a highly shear thinning behaviour under increasing stress. Not much difference can be seen between the meat being dried with and without ultrasound for either the hot air or the cold air-dried sample. In figure 53 all 4 is compared together. The 2 cold air-dried meats appear to have formed pastes with higher viscosity than the hot air-dried meats. The effect of the ultrasound during the drying cannot be determined. The shear thinning behaviour appears to be behaving similar, but the viscosity for some pastes are consistently higher than others. The difference in viscosity might be due to small differences in the formulation, or possibly the slight difference in initial moisture content of the meat used. The cold air-dried meat might rehydrate more efficiently, lower the water content for the continuous phase of the paste and thus increasing its viscosity.

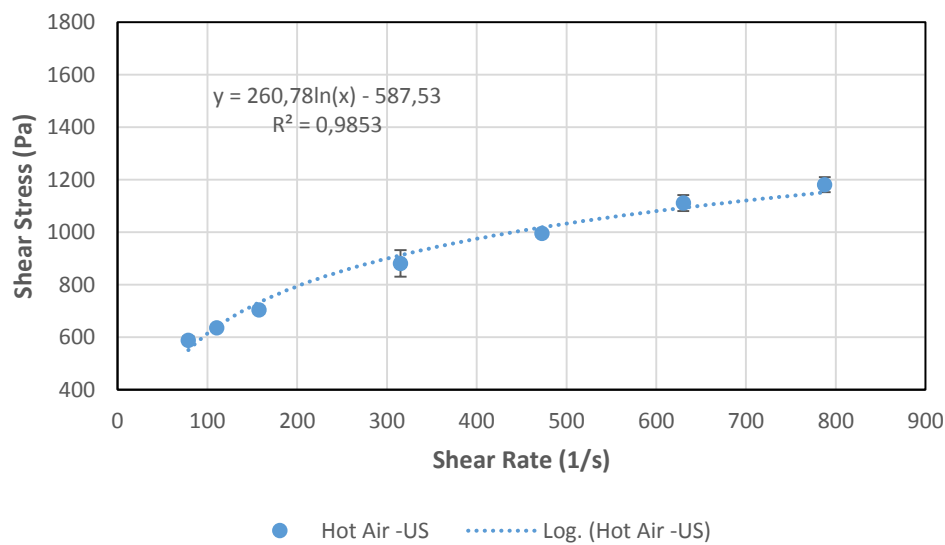


Figure 49 The flow curve for hot air-dried meat without ultrasound.

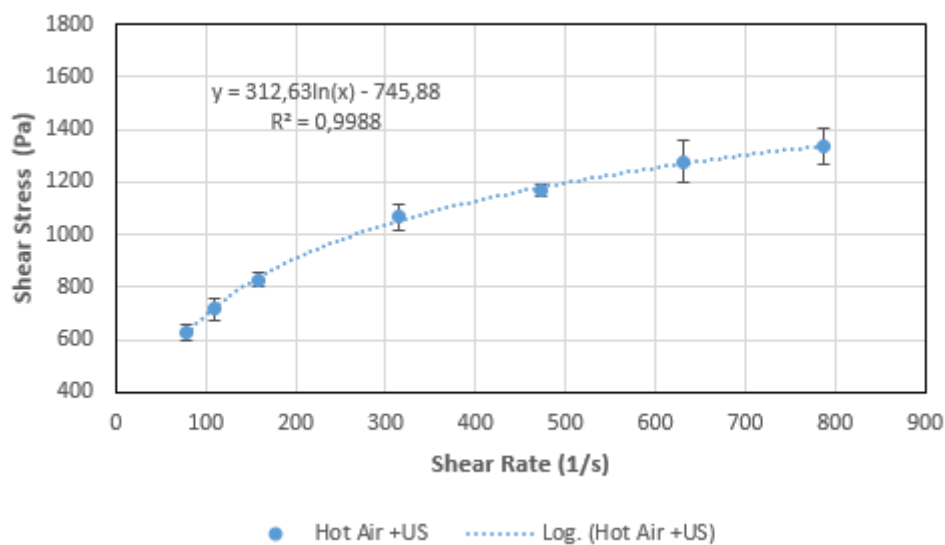


Figure 50 The flow curve for hot air-dried meat with ultrasound.

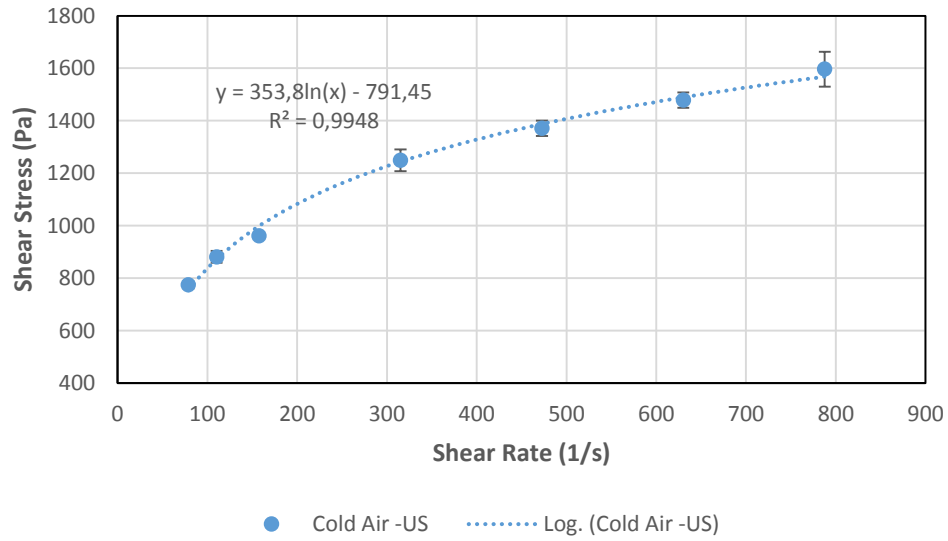


Figure 51 The flow curve for cold air-dried meat without ultrasound.

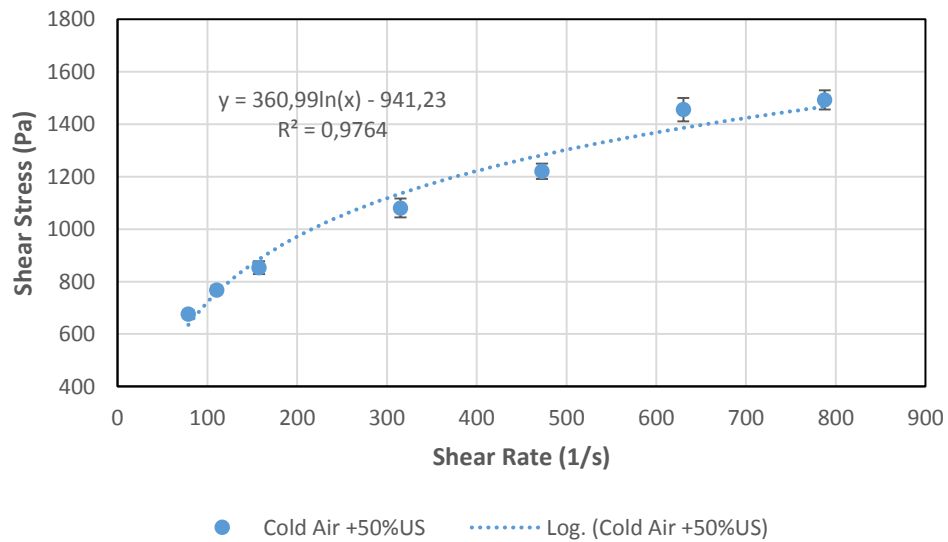


Figure 52 The flow curve for cold air-dried meat with 50% ultrasound power.

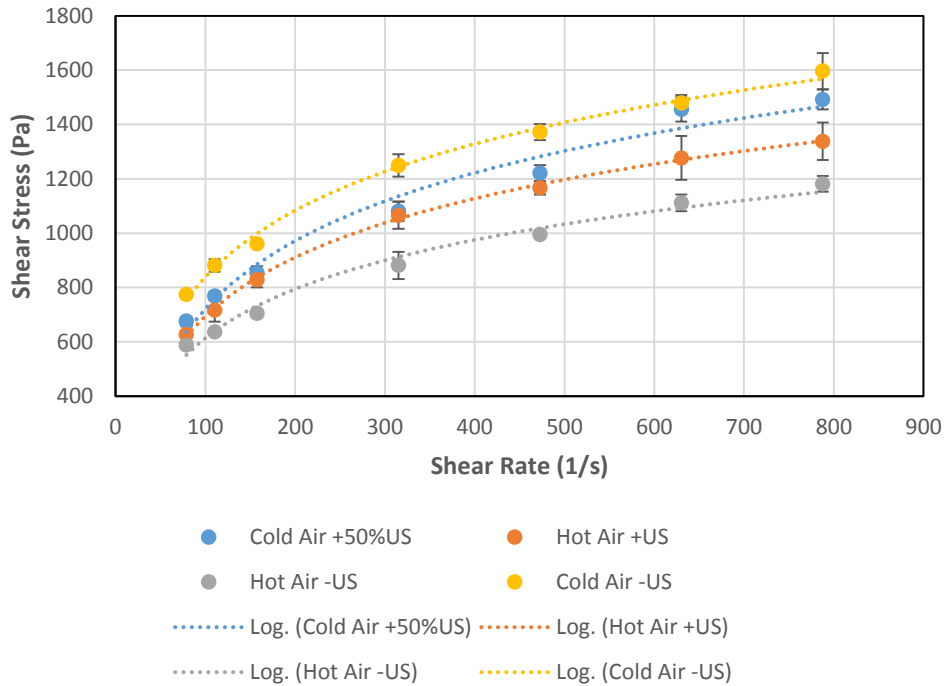


Figure 53 The flow curve for hot air-dried meat with and without ultrasound and cold air-dried meat with 50% ultrasound power and without.

6.10.3 Drying Method: Particle size

The particle sizes of the different pastes can be seen in figure 54. The pastes formulated with meat dried using with or without ultrasound were very similar in their particle size distribution. A slight difference though can be seen between the meat dried using hot or cold air. The pastes containing hot air-dried meat powder has a portion of particles that are larger than in the cold air-dried pastes.

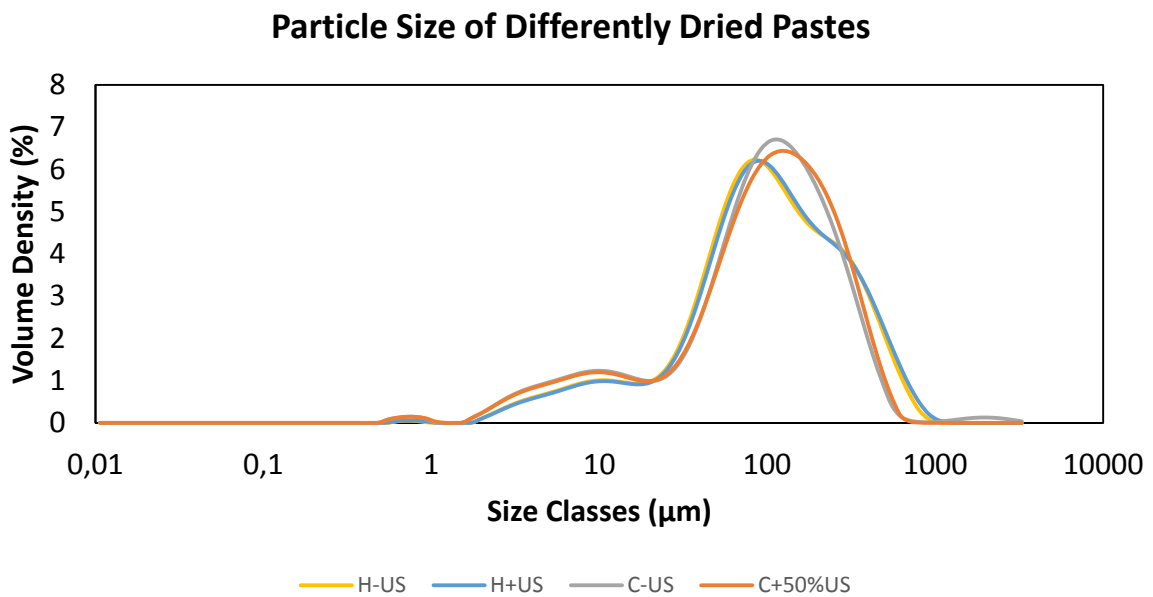


Figure 54 Size distribution of the differently dried meat pastes. H+US = hot air with ultrasound, C-US = cold air without ultrasound and C+50%US = cold air with 50% ultrasound power.

The dry powders of the differently dried meats were analysed in the Mastersizer 3000s Aero unit. It provided data that the hot air-dried powder particles were generally slightly smaller than the cold air-dried particles, which can be seen in figure 55. During the measurement though, it looked like the particles were sticking together, and more so for the cold air-dried particles. The same analysis was done by dispersing the particles in water and then measure their size using the Mastersizer 3000s Hydro unit, which can be seen in figure 56. The results better correlated with the measurement of the size distribution of the particles pastes. The hot air-dried powders contained a fraction of particles that were slightly larger than the cold air-dried powder.

Particle Size of Differently Dried Powders

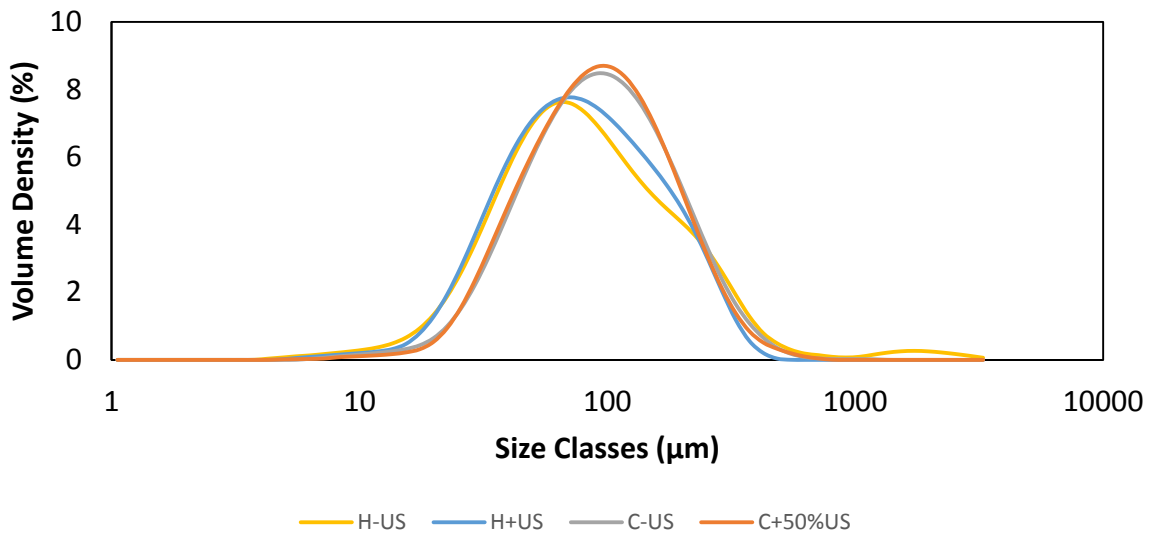


Figure 55 Size distribution of the differently dried meat powders. H+US = hot air with ultrasound, C-US = cold air without ultrasound and C+50%US = cold air with 50% ultrasound power.

Particle Size of Differently Dried Powders in Water

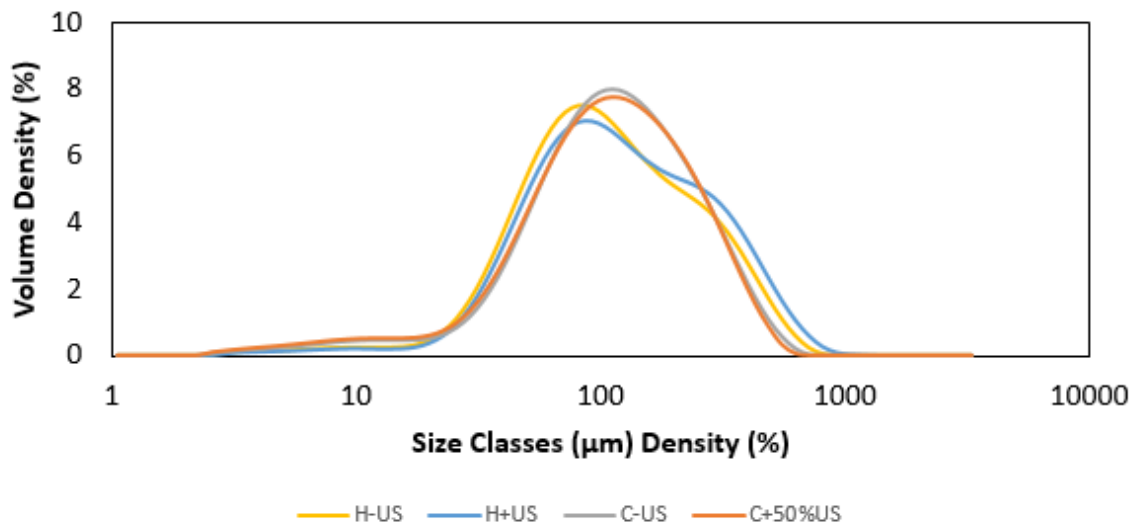


Figure 56 Size distribution of the differently dried meat powders dispersed in water. H+US = hot air with ultrasound, C-US = cold air without ultrasound and C+50%US = cold air with 50% ultrasound power.

6.10.4 Drying Method: Structure

The 4 pastes were looked at through the digital microscope which can be seen on figure 57. No difference was detected.

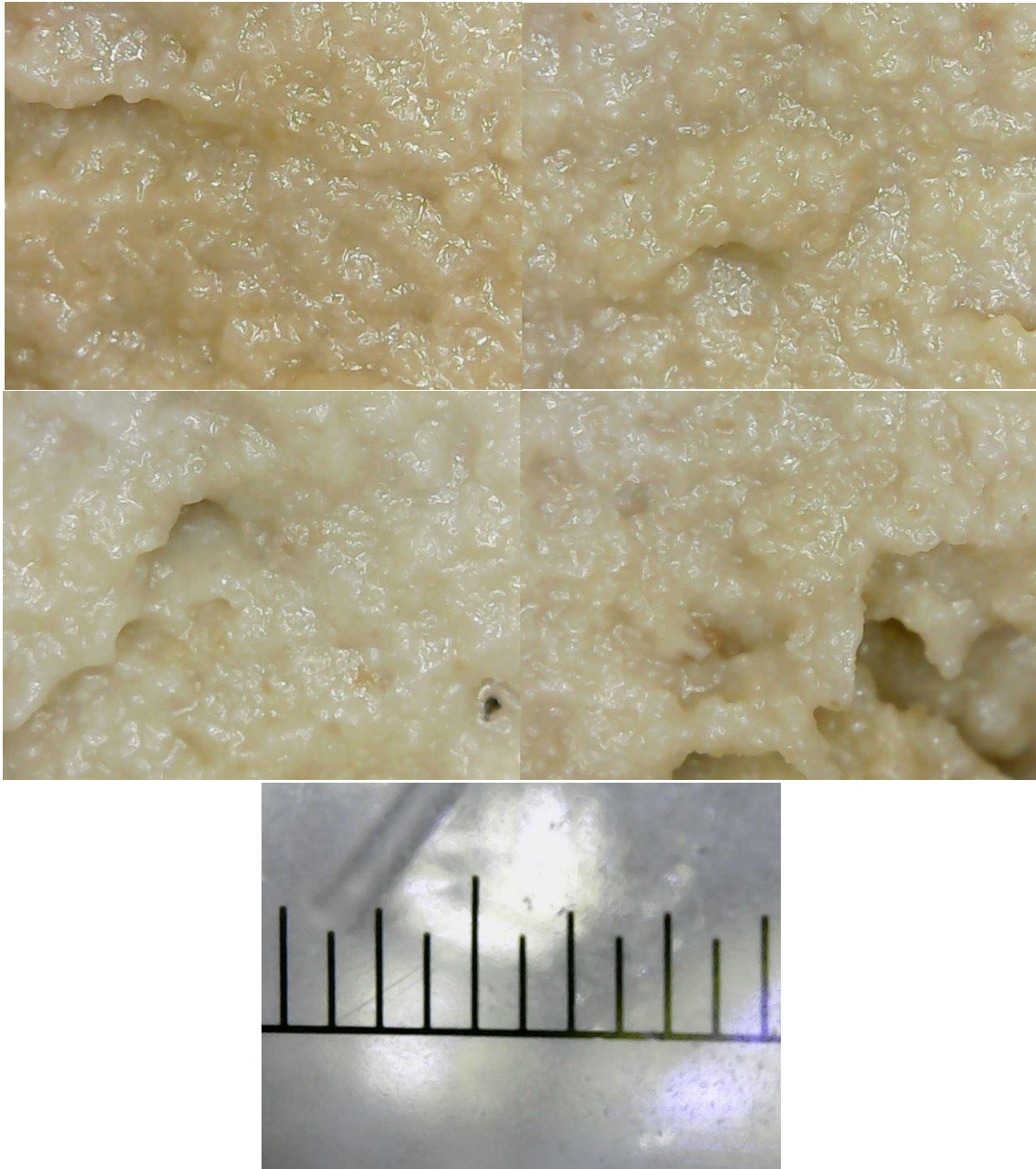


Figure 57 Differently dried meats. Top left: hot air without US, top right: hot air with US, bottom left: cold air without US, bottom right: cold air with US (50% power) and bottom: ruler, every gap represents 0.5mm.

6.10.5 Drying Method: Printing

The printed figures using the 4 different pastes can be seen in figure 58. There was no visible or textural difference between the prints. Regarding though that their behaviours was slightly different in the results from the analysis methods indicates that the difference found was not large enough to be detected while printing.

Thus, the paste created using the cold-air dried meat where slightly favourable for printing purposes since the general viscosity was slightly higher, and the higher viscosity enabled the layers to be printed without the figure slumping. The ultrasound did not have an impact on the properties of the meat that was measured in the work. Since the ultrasound did not affect the paste, the meat dried with ultrasound was favourable since the ultrasonic transducer decreased the drying time and thus also the energy consumption and cost of drying. Even more so considering that the ultrasound should have an ever greater impact while drying at lower temperatures, and lower temperatures almost was an necessity because the higher temperatures created a meat that was extremely difficult to mill.

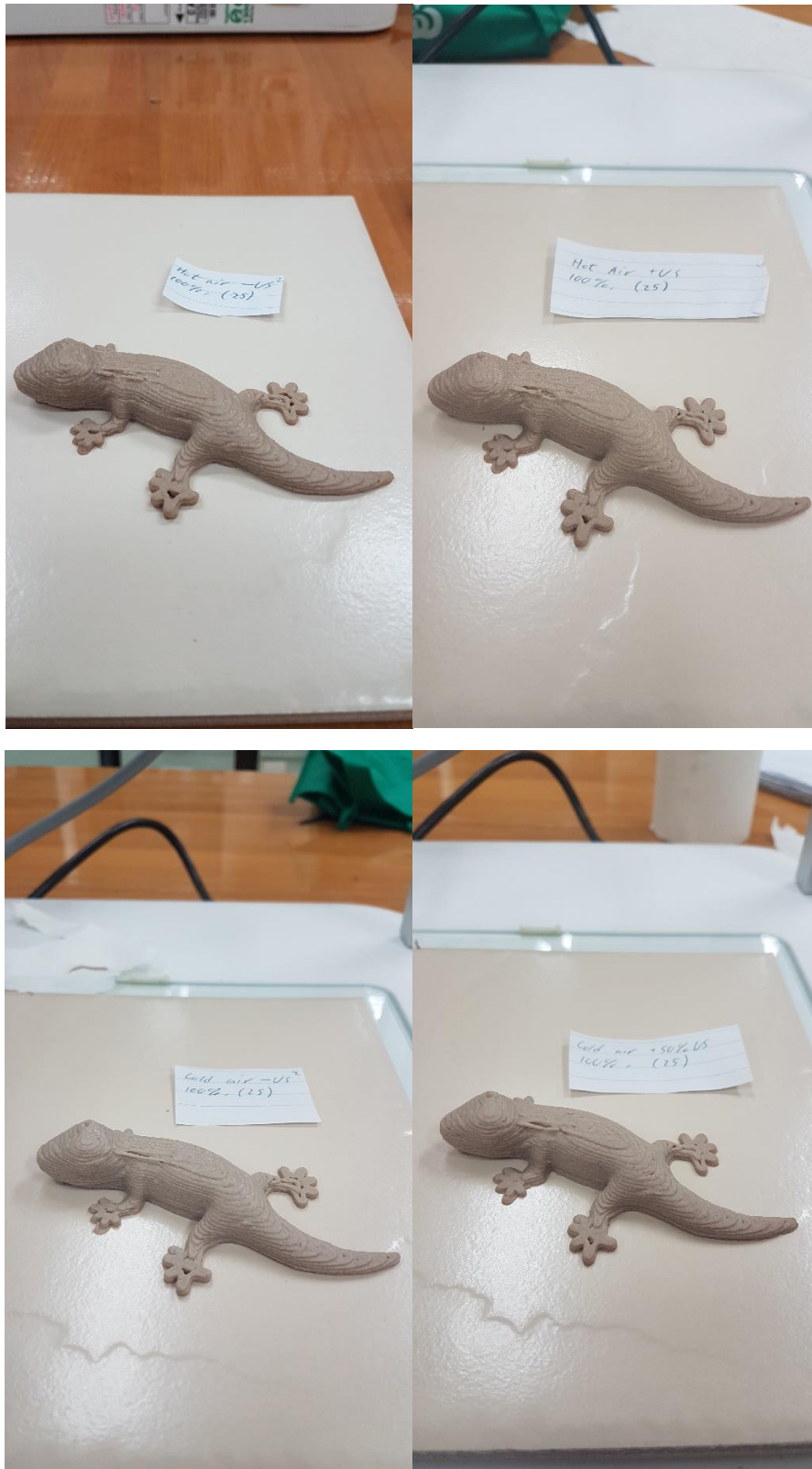


Figure 58 Differently dried meats. Top left: hot air without US, top right: hot air with US, bottom left: cold air without US and bottom right: cold air with US (50% power).

7 CONCLUSION

The aim of this master thesis was to investigate the impact of ultrasonics, by a new ultrasonic transducer on which a patent application has been filed by CSIRO, on drying kinetics of ground beef at both 40°C and -15°C. It was additionally to investigate the drying methods impact on the printability of the meat. It was determined that the ultrasonic assisted drying greatly increased the drying speed at both 40°C and -15°C. At 40 °C the drying time was roughly shortened by 40%, though more work needs to be conducted in order to investigate the impact at -15°C because the cooling pump used in the report was not strong enough to properly pump enough coolant to cool the transducer to the desirable temperature of -15°C.

Both meats dried using hot and cold air and is printable, if the particles size is reduced enough and mixed with proper thickener. It is a lot easier to mill meat that has been dried using lower temperatures because it is more porous than the hot air-dried meat in which the surface closes and hardens. Powerful mills are required to mill hot air-dried meat enough for it to be printable, often requiring more time due to heat from friction in the mill that needs to cool down. Several mills investigated were not able to mill the hot air-dried meat sufficiently. Even when the particle size was reduced enough, the paste created using the cold air-dried meat displayed a slightly higher viscosity. Thus, using colder temperatures while drying meat for printing purposes is highly favourable.

Barely any difference was detected between meat dried with or without ultrasound in terms of textural properties, how easily the particle size was reduced, or properties of the pastes created with the different powders.

It can be determined that due to the vast improvement in structural properties of the food dried using lower temperatures and that adding ultrasound during the drying has not proved to alter the product, hence using ultrasound to assist drying is favourable. The ultrasound greatly facilitates drying kinetics, reducing the time the material is needed to be exposed to hot air and thus improving product quality and process speed. Less energy would also be required and thus implementing ultrasound during drying would then reduce cost in several areas.

8

FURTHER WORK

The pump for the cooling agent was not strong enough to pump enough refrigerant to properly cool the transducer during the drying at -15°C , leading to that the sample was slightly heated. It did not seem to affect greatly, but to prove that the transducer increases drying speeds at temperatures below freezing, another test should be conducted once the new pump arrives. Work is now on the way to soon create a pilot scale version of the transducer. Hopefully analysis of the nutrients of the freeze-dried meat will show that the decrease of drying time when utilising ultrasound improves the nutritional content of the meat.

It was found that pea protein powder in water at a concentration of around 25% mass to water was easily printed without additives. Further work could investigate the printability of pea protein pastes and mixtures of pea protein with other foods for addition of nutrients. Also, to use pea protein as thickener to pastes with too low viscosity.

The work on the formulation of the printable pastes has focused on minced beef but could be potentially be applied to other sources of proteins as well, such as plant or insect-based proteins.

The transglutaminase did not arrive in time to be utilised as a thickener during the work. Future work could be conducted in investigating transglutaminase as a thickener when printing protein-based pastes.

The work done on investigating the printability of the pastes was focused in the comparison of the differently dried meats. If more detailed data is required on the properties of printable pastes, then more thorough work investigating the viscosity and yield stress of pastes should be conducted.

Finally, the importance of a proper yield stress in a printable paste was realized after the measurements had been conducted. In further work the yield stress ought to be better investigated and determined.

9 REFERENCES

- [1] J. Gamboa-Santos, A. Montilla, J. Andrés Cárcel, M. Villamiel, J. V. Garcia-Perez, "Air-bourne ultrasound application in the convective drying of strawberry," *Journal of Food Engineering*, vol. 128, pp. 132-139, 2014.
- [2] L. M. Diamante, P. A. Munro, "Mathematical modelling of hot air drying of sweet potato slices," *Internutional Journal of Food Science and Technology*, vol. 26, pp. 99-109, 1991.
- [3] E. Tsotsas, T. Metzger, V. Gnielinski, E. Schlünder, Drying of Solid Materials, in Ullmann's Encyclopedia of Industrial Chemistry. B. Elvers, Weinheim, Germany: Wiley-VCH, 2010.
- [4] W. R. W. Daud, M. H. Ibrahim, M. Z. M. Talib, "PARAMETER ESTIMATION OF FICK'S LAW DRYING EQUATION," *Drying Technology*, Vols. 15:6-8, pp. 1673-1686, 1997.
- [5] E. Shahraeeni, P. Lehmann, D. Or, "Coupling of evaporative fluxes from drying porous surfaceswith air boundary layer:Characteristics of evaporation from discrete pores," *WATER RESOURCES RESEARCH*, vol. 48, pp. 1-15, 2012.
- [6] G. V. Barbosa-Cánovas, J. J. Fernández-Molina, S. M. Alzamora, M. S. Tapia, A. López-Malo, J. W. Chanes , Handling and Preservation of Fruits and Vegetables by Combined Methods for Rural Areas, Rome: FOOD AND AGRICULTURE ORGANIZATION OF THE UNITED NATIONS, 2003.
- [7] C. Ratti, "Hot air and freeze-drying of high-value foods: a review," *Journal of Food Engineering*, vol. 49, no. 4, pp. 311-319, 2001.
- [8] P. Lopez-Buesa, T. J. Mason, E. Riera, A. Vercet, "Application of Ultrasound," *Emerging Technologies for Food Processing*, vol. 1, pp. 323-351, 2005.
- [9] T.J. Mason, F. Chemat, M. Ashokkumar, "Power ultrasonics for food processing," *Annual Review of Food Science*, vol. 5, pp. 263-284, 2014.
- [10] P. Larysa, "Application of Ultrasound," *Emerging Technologies for Food Processing, 2nd edition*, vol. 2, pp. 271-291, 2014.
- [11] J. A. Cárcel, J. V. García-Pérez, J. Bedito, A. Mulet, "Food Process Innovation Through New Technologies: Use of Ultrasound," *Journal of Food Engineering*, vol. 110, pp. 200-207, 2012.
- [12] J. V. García-Pérez, J. A. Carcel, A. Mulet, E. Riera, J .A. Gallego-Juarez, , "29 - Ultrasonic drying for food preservation," *Power Ultrasonics - Applications of High-Intensity Ultrasound*, pp. 875-910, 2015.
- [13] H. T. Sabarez, J. A. Gallego-Juarez, E. Riera, "Ultrasonic-Assisted Convective Drying of Apple Slices," *Drying Technology: An International Journal,,* vol. 30, pp. 989-997, 2012.
- [14] A. Mulet, J. A. Cárcel, J. V. García-Pérez, E. Riera, "Ultrasound-Assisted Hot Air Drying of Foods," *Ultrasound Technologies for Food and Bioprocessing*, pp. 511-534, 2010.

- [15] J. V. García-Pérez, J. A. Cárcel, E. Riera, A. Mulet, , "Influence of the applied acoustic energy on the drying of carrots and lemon peel," *Drying Technology*, vol. 27, p. 281–287, 2009.
- [16] K. F. Graff, "Power ultrasonic transducers: principles and design," *Power Ultrasonics: Applications of High-Intensity Ultrasound*, vol. 1, pp. 127-128, 2015.
- [17] J. A. Gallego-Juarez, K. F. Graff, "Introduction to power ultrasonics," *Power Ultrasonics: Applications of High-Intensity Ultrasound*, vol. 1, pp. 1-5, 2015.
- [18] J. A. Gallego-Juarez, G. Rodriguez, V. M. Acosta-Aparicio, E. Riera, A. Cardoni, "Power Ultrasonic transducers with vibrating plate radiators," *Power Ultrasonics*, pp. 159-193, 2015.
- [19] J. I. Lipton, M. Cutler, F. Nigl, D. Cohen, H. Lipson, "Additive manufacturing in the food industry," *Trends in Food Science and Technology*, vol. 43, pp. 114-123, 2015.
- [20] J. Sun, W. Zhou, L. Yan, D. Huang, L. Lin, "Extrusion-based food printing for digitalized food design and nutrition control," *Journal of Food Engineering*, vol. 220, pp. 1-11, 2018.
- [21] C. L. Tohic, J. J. O'Sullivan, K. P. Drapala, V. Chartrin, T. Chan, A. P. Morrison, J. P. Kerry, A. L. Kelly, "Effect of 3D printing on the structure and textural properties of processed cheese," *Journal of Food Engineering*, vol. 220, pp. 56-64, 2017.
- [22] F. C. Godoi, S. Prakash, B. R. Bhandari, "3d printing technologies applied for food design: Status and prospects," *Journal of Food Engineering*, vol. 179, pp. 44-54, 2016.
- [23] Z. Liu, M. Zhang, B. Bhandari, C. Yang , "Impact of rheological properties of mashed potatoes on 3D printing" , ,," *Journal of Food Engineering*, vol. 220, pp. 76-82, 2017.
- [24] H. W. Kim, H. Bae, H. J. Park, "Reprint of: Classification of the printability of selected food for 3D printing: Development of an assessment method using hydrocolloids as reference material," *Journal of Food Engineering*, vol. 220, pp. 28-37, 2018.
- [25] A. Dick, B. Bhandari, S. Prakash, "3D Printing of meat," *Meat Science*, vol. 153, pp. 35-44, 2019.
- [26] M.Motoki, K.Seguro, "Transglutaminase and its use for food processing," *Trends in Food Science & Technology*, vol. 9, no. 5, pp. 204-210, 1998.
- [27] C. Kuraishi, K. Yamazaki, Y. Susa, "TRANSGLUTAMINASE: ITS UTILIZATION IN THE FOOD INDUSTRY," *Food Reviews International* , vol. 17, no. 2, pp. 221-246, 2001.
- [28] K. I. Draget, "29 - Alginates," *Handbook of Hydrocollids (Second edition)*, vol. 2, pp. 807-828, 2009.
- [29] E. Onsøyen, "Alginates," in *Thickening and Gelling Agents for Food*, Boston, Springer, 1997, pp. 22-44.
- [30] b. Katzbauer, "Properties and applications of xanthan gum," *Polymer Degradation and Stability* , vol. 59, no. 1-3, pp. 81-84, 1998.

- [31] F. García-Ochoa, V.E. Santos, J.A. Casas, E. Gómez, "Xanthan gum: production, recovery, and properties," *Biotechnology Advances*, vol. 18, no. 7, pp. 549-579, 2000.
- [32] P. J. Whitcomb, C. W. Macosko, "Rheology of Xanthan Gum," *Journal of Rheology*, vol. 22, no. 493, pp. 493-505, 1978.
- [33] M. Bourne, *Food Texture and Viscosity, Concept and Measurement*. 2nd Ed., New York: Academic Press, 1982.
- [34] C. D. Rielly, *Food Rheology*, in *Chemical Engineering for the Food Industry*, Boston: Springer, 1997.
- [35] M. Alveteg, *Handbook*, Department of Chemical Engineering, Lund: Lund University, 2015.
- [36] R. Darby, *Fluid Properties in Perspective*, in *Chemical Engineering Fluid Mechanics*, 2nd Ed., New York: Marcel Dekker, Inc., 2001.
- [37] L. H. Sperling, *Introduction to Physical Polymer Science*, Hoboken, New Jersey: John Wiley & Sons, 2006.
- [38] J. A. Manson, *Polymer Blends and Composites*, New York: Springer US, 1976.
- [39] R. C. Hibbeler, *Stress*, in *Mechanics of Materials*, 8th Ed. M. Horton, Boston: Pearson Prentice Hall, 2011.